

1 **Palaeogeographic reconstructions of western New Guinea from**
2 **biostratigraphic data**

3 D. Gold¹, L White¹, I. Gunawan^{1,2}, M. Boudagher-Fadel³

4

5 1. Southeast Asia Research Group, Department of Earth Sciences, Royal Holloway University
6 of London, Egham, Surrey, TW20 0EX

7 2. Institut Teknologi Bandung, Bandung, Indonesia...

8 3. Department of Earth Sciences, University College London, Gower Street, London, WC1E
9 6BT, UK

10

11 **Abstract**

12 New biostratigraphic analyses of approximately 200 outcrop samples and
13 reinterpretation of the biostratigraphy nearly 100 wells distributed across Indonesian
14 western New Guinea enables reconstruction of the palaeogeography of the region
15 from the Silurian to present day. Biostratigraphic ages and palaeodepositional
16 environments were interpreted predominantly from occurrences of planktonic and
17 larger benthic foraminifera. Palaeogeographic reconstructions reveal two major
18 transgressive-regressive cycles in regional relative sea-level with peaks interpreted
19 to occur in the Late Cretaceous and Late Miocene. During the Late Paleozoic and
20 Early Mesozoic terrestrial deposition was prevalent across much of western New
21 Guinea as it formed part of the northern promontory of the Australian continent,
22 termed the Sula Spur. From the Late Jurassic the first regional transgressive event
23 resulted in increasing water depths until the Late Cretaceous. Carinate planktonic
24 foraminifera are widespread in sediments of this age encountered in wells and
25 outcrop across the entire region. A regressive event from the Late Cretaceous into
26 the Paleogene resulted in widespread shallow water carbonate platform deposition

27 by the Middle to Late Eocene. A minor transgressive event is recorded during the
28 Oligocene but was cut short by collision between the Australian continent and intra-
29 Pacific island arcs in the Early Miocene causing regional uplift in the region and
30 formation of a subaerial unconformity. Following uplift, carbonate platforms
31 established in shallow water areas depositing youngest units of the New Guinea
32 Limestone Group. A second transgressive event, initiating during the Middle
33 Miocene, reached its peak in the Late Miocene this was followed by a further
34 regression culminating in the present day topographic expression of western New
35 Guinea.

36

37 **Keywords:** New Guinea; planktonic; larger benthic; foraminifera; paleogeography

38

39 **1. Introduction**

40 New Guinea represents the northernmost boundary of the Australian Plate and has
41 done at least as far back as the Permian when New Guinea was part of an Andean-
42 style arc system that extended around a large portion of Gondwana (Hill and Hall
43 2003; Hall 2002; 2012; Metcalfe 2009; Gunawan et al., 2012; 2014; Webb and
44 White, 2016). This long-lived plate boundary records evidence of numerous
45 accretion events and pulses of magmatism and metamorphism during the Eocene,
46 Oligocene, Miocene and Pliocene (Baldwin et al., 2012; Baldwin and Ireland; Davies
47 – Review; Pieters et al., 1983; Visser and Hermes, 1962; Pigram; Jaques). However,
48 much of the geology of New Guinea is also dominated by carbonate deposition
49 during seemingly long periods of quiescence (Pieters et al., 1983; Pigram; Visser
50 and Hermes, 1962; Hill; Davies; Baldwin et al., 2012). In this paper we present new
51 biostratigraphic age data based on benthic and planktonic foraminifera as well as

52 facies analyses from nearly 200 outcrop samples and 100 wells from western New
53 Guinea. The aim of this work was to better establish the duration and facies
54 distribution of carbonate deposition to better understand periods of quiescence at the
55 northern margin of the Australian Plate between the Silurian and present day.

56

57 1.1 The Bird's Head, Neck, Body and Tail

58 New Guinea is often described to reflect the shape of a bird, comprising the Bird's
59 Head, Neck, Body, and Tail from west to east, respectively (Fig. 1). The Bird's Head,
60 Neck and part of the Body make up the Indonesian provinces of West Papua and
61 Papua (formerly known as Irian Jaya). The rest of the Bird's Body and Tail make up
62 Papua New Guinea. The island's peculiar morphology largely reflects the geology
63 and tectonic evolution of the island. For example, the Bird's Neck is largely
64 composed of limestones and siliciclastic rocks shortened during the development of
65 the Lengguru Fold and Thrust Belt. These deformed rocks form part of a mountain
66 belt that extends from eastern New Guinea (the Bird's Head), along the Central
67 Range (the Bird's Body) to the eastern tip of the island (Bird's Tail) (Fig. 1). This
68 paper focuses primarily on the stratigraphic and paleogeographic evolution of the
69 Bird's Head, Neck and Body.

70

71 1.2 Geological Mapping of Western New Guinea

72 The first comprehensive geological mapping of Indonesian New Guinea was
73 conducted between 1935 and 1960 by geologists of the Nederlandsche Nieuw
74 Guinee Petroleum Maatschappij and is described in great detail by Visser and
75 Hermes (1962). While this work was completed before the advent of the theory of
76 plate tectonics, the observations that are reported in this work are extremely valuable

77 and lay the foundation for the stratigraphy of Irian Jaya. This work was later refined
78 by the Indonesian Department of Mining and Energy's Geological Research and
79 Development Centre (GRDC) and the Australian Bureau of Mineral Resources (now
80 known as Geoscience Australia) as part of the Irian Jaya Geological Mapping Project
81 between 1978 and 1982; the results of which are summarised in Pieters et al.
82 (1983).

83

84 Pieters et al (1983) described the stratigraphy of the Bird's Head as consisting of
85 three provinces. To the north lies an Oceanic Province of ophiolite and island arc
86 volcanics of Pacific Plate affinity separated from a southern Continental Province of
87 Australian continental affinity separated by a Transition Zone of deformed and
88 metamorphosed rocks (Pieters et al., 1983). The Transition Zone represents a suture
89 marking the collision of the Australian continent with the island arc on the Pacific
90 Plate in the early Miocene (Fig. 1), with continued convergence to this day (Pieters et
91 al., 1983; Milsom, 1992). Thus the stratigraphy of the Bird's Head can be broadly
92 described as intra-Pacific island arc material to the north and east, and Australian
93 continental material to the south and west, the post-collisional stratigraphy of both
94 domains is reasonably contiguous (Fig. 2). In this paper we focus on carbonates
95 deposited on both the former intra-Pacific island arc and Australian continent.

96

97 **2. Depositional History of western New Guinea sediments**

98

99 The oldest strata within the Bird's Head are found in rocks of Australian continental
100 affinity. The Kemum Formation forms a basement block of metamorphosed fine-
101 grained siliciclastic rocks assigned a Silurian-Devonian age based on the presence

102 of graptolites (Visser and Hemres, 1962; Pieters et al., 1983). Both the Kemum and
103 Aisasjur Formations are reported to comprise distal and proximal turbidite deposits,
104 respectively (Visser and Hermes, 1962; Pieters et al., 1983; Webb and White, 2016).
105 The Modio Dolomite of the Central Ranges is the oldest carbonate unit deposited
106 from the Silurian-Devonian (Fig. 2; Pieters et al., 1983). The Carboniferous to
107 Permian was a period of relatively stable paralic sediment deposition, with
108 occasional shallow marine incursions marked by thin limestone beds in the Central
109 Ranges. The Permo-Carboniferous Aifam Group contains various terrestrial and
110 marine deposits. In this group the Aimau, Ainim and Aiduna formations are reported
111 to contain conglomerates, red beds and coal seams suggesting a terrestrial
112 depositional setting, the Aifat mudstone however may have been deposited in a
113 basinal setting (Pieters et al., 1983).

114

115 During the Triassic only arid terrestrial deposits of the Tipuma Formation are known
116 from the Bird's Head, with the nearest known carbonates of this age found in the
117 Late Triassic Manusela and Asinepe Limestone formations of Misool and Seram
118 (Pieters et al., 1983; Martini et al., 2004). Here, early to mid Jurassic calcareous
119 sediments were deposited in shallow seas with little siliciclastic input, however, in the
120 Bird's Head deposition of siliciclastic material forming the Tamrau Formation and
121 Kembelangan Group, persisted throughout the Jurassic and into the Late
122 Cretaceous (Fig. 2).

123

124 The Cretaceous siliciclastic units of the Kembelangan Group include the Jass
125 Formation, Piniya Mudstone and the Woniwogi and Ekmai Sandstones. Carbonate
126 deposits in the Bird's Head are not known until the Late Cretaceous (Pieters et al.,

127 1983) where Coniacian to Maastrichtian age siliciclastics of the Ekmai Sandstone
128 pass laterally into the deep-water pelagic carbonates of the Simora Formation (Fig.
129 2; Brash et al., 1991). Fragments of inoceramid bivalves within the base of the
130 conformably overlying Waripi Formation suggest a Late Cretaceous age.

131

132 From the Late Cretaceous and into the Paleogene there is a distinct change from
133 siliciclastic to carbonate deposition recorded across the Bird's Head. Visser and
134 Hermes (1962) proposed the 'New Guinea Limestone Group' (NGLG) to include Late
135 Cretaceous to Middle Miocene limestones, between 1km and 1.6km thick, that
136 outcrop in the western Bird's Head, through the Lengguru Fold and Thrust Belt, into
137 the Central Range and Papua New Guinea (Brash et al., 1991). The oldest
138 Paleogene strata of the NGLG, the Waripi Formation, were deposited in shallow-
139 water areas of a new Cenozoic basin from the Mid to Late Paleocene (Brash et al.,
140 1991; Fig. 2). Brash et al. (1991) suggest that in deep-water areas to the north of this
141 new basin, the Imskin Limestone may interfinger with the Waripi Formation (Fig. 2).
142 The Cenozoic basin was relatively stable throughout the Eocene, depositing the
143 shallow-water Faumai and Lengguru Limestones, while the Imskin Limestone
144 continued accumulating pelagic carbonate up until collision with the intra-Pacific
145 island arc in the Early Miocene (Fig. 2).

146

147 Within the intra-Pacific island arc, carbonate deposition was restricted to patch reefs
148 developed around eroded volcanoes known from the Eocene age Auwewa
149 Formation (Fig. 2), up until the time of collision (Wilson, 2002). Following collision in
150 the early Miocene, carbonate platform development was widespread across much of
151 the Bird's Head. Early to Middle Miocene platform carbonates of the Kais and Maruni

152 Limestones, and Wainukendi and Wafordori Formations (Fig. 2), were subsequently
153 drowned during a Mid to Late Miocene transgressive event that terminated platform
154 accumulation abruptly (Brash et al., 1991; Gold et al., in review). During the
155 Pliocene, or very latest Miocene, rapid uplift attributed to major thrusting, folding
156 (Wilson, 2002) and strike-slip faulting prevailed in the Bird's Head causing the
157 formation of several basins (Pieters et al., 1983). Erosion of uplifted areas filled
158 these basins with much siliciclastic sediment. Only the islands of Misool and Biak
159 remained starved of siliciclastic sedimentation permitting deposition of platform
160 carbonates of the Wardo, Korem and Mokmer Formations (Fig. 2) in the relatively
161 clear waters (Pieters et al., 1983; Wilson, 2002).

162

163 **3. Methodology**

164 This paper presents the results of several field campaigns conducted by the
165 Southeast Asia Research Group (SEARG), Royal Holloway, University of London, in
166 the Bird's Head of Indonesian New Guinea. Over these campaigns nearly 200
167 samples were collected of the New Guinea Limestone and associated carbonate
168 units.

169 Samples were thin sectioned and examined for carbonate petrography and
170 biostratigraphic dating using planktonic and larger benthic foraminifera, of these 198
171 samples yielded well-constrained biostratigraphic ages. Ages are assigned using
172 planktonic foraminiferal zones of Blow (1979), Berggren and Miller (1988) and
173 Berggren et al. (1995), recalibrated to Wade et al.'s (2010) sub-tropical planktonic
174 foraminiferal zones. Larger benthic foraminiferal zones are assigned to the Indo-
175 Pacific 'letter stages' of Adams (1965, 1970). We subdivided the biostratigraphic

176 results into 19 time intervals to show the paleogeographic evolution of western New
177 Guinea between the Silurian and Pleistocene.

178

179 Palaeogeographic reconstructions were determined using bathymetric preferences
180 of organisms (Hallock and Glenn, 1986; van Gorsel, 1988; Murray, 2006;
181 BouDagher-Fadel, 2008; 2015; Beavington-Penney and Racey, 2004; Lunt, 2013)
182 observed in each sample, summarised in Figure 4. For simplicity in generating the
183 palaeogeographic maps, five relative bathymetries were assigned to samples
184 containing depth-diagnostic foraminiferal assemblages (Fig. 4). Where
185 heterogeneous depositional environments were interpreted at a single locality, the
186 modal depositional setting for that time and location is recorded in the gross
187 depositional maps.

188

189 In addition to the new analyses of samples collected across the Bird's Head,
190 biostratigraphic data from 97 wells in the region were reviewed and reinterpreted.
191 Stratigraphic intervals within the wells were assigned to the relative bathymetry
192 scheme using records of foraminiferal occurrences that meet the criteria laid out in
193 Figure 4. Well data used in this study were sourced from a combination of the public
194 domain and SEARG confidential industry data; consequently we are unable to show
195 the location of all wells.

196

197 The depositional bathymetries of samples and well intervals interpreted for each time
198 slice were plotted using ArcGIS software so that the spatial distribution of facies
199 could be compared with existing geological maps of the region produced by the
200 GRDC. We used the maps and our new data to draw gross depositional environment

201 maps. These were overlain on the present day configuration of the Bird's Head to
202 show where deepening/shallowing trends can be observed today. The facies maps
203 were plotted according to the present day configuration of western New Guinea, but
204 do not attempt to restore the displacement of faults or large-scale rotation of
205 continental fragments (e.g. Hall 2012; Charlton, 2010). While these maps are
206 somewhat simplified in terms of the region's tectonic history, our aim was to produce
207 a series of maps that could be used to identify the present day distribution of
208 potential hydrocarbon plays.

209

210 **4. Palaeogeographic reconstructions**

211

212 4.1 Temporal Trends

213 Through the reconstruction of palaeodepositional environments using microfossil
214 assemblages, temporal trends of relative sea-level change can also be deduced.
215 Figure 5 displays a localised relative sea-level curve for the Bird's Head region from
216 the Silurian to Pleistocene, based on the palaeogeographic reconstructions of an
217 arbitrary data point within the northern Bintuni bay.

218

219 Relative sea-level fall during the Silurian saw the replacement of deep water settings
220 to terrestrially dominated environments persisting from the Permian to Early Jurassic
221 (Fig. 5). Transgression throughout the Middle Jurassic and into the Cretaceous
222 resulted in peak Mesozoic relative sea-level by the Late Cretaceous (Fig. 5) and the
223 deposition of many fine-grained siliciclastic formations. Relative sea-level fell
224 throughout the Paleogene until the Middle to Late Eocene when widespread
225 shallow water areas permitted the growth of extensive carbonate platforms

226 represented by the oldest units of the NGLG including the Faumai, Lengguru and
227 Imskin Limestones, and lenses within the Auwewa Formation.

228

229 Relative sea-level increased for a short duration during the Oligocene before the
230 onset and perpetuation of arc-continent collision between the Australian and Pacific
231 Plates in the earliest Miocene (Fig. 2). This collision caused sub-aerial erosion of
232 Paleogene sediments in some areas forming a regional Early Miocene unconformity
233 (Fig. 2). Collisional uplift within other areas, resulting in regional relative sea-level fall
234 (Fig. 5), permitted renewed widespread carbonate platform growth and deposition of
235 Early Miocene units of the NGLG.

236

237 Stable shallow-water carbonate deposition of the NGLG continued for at least 6 Myr
238 across much of western New Guinea until a second regional transgressive event
239 initiated in the Middle Miocene (Fig. 5). Relative sea-level rise reached its peak in the
240 Late Miocene, possibly correlating the global Tor1 flooding event (Gold et al., in
241 review), resulting in the deposition of widespread deep-water limestones and fine-
242 grained siliciclastics of the Klasafet and Klasaman Formations. Relative sea-level
243 began to fall again during the Pliocene and continued until the present day (Fig. 5),
244 leaving western New Guinea sub-aerially exposed as we know it today.

245

246 4.2 Silurian

247 During the Silurian, bathymetries in excess of 100m are interpreted across much of
248 the central Bird's Head (Fig. 6). This interpretation is based on published
249 descriptions and distribution of the widespread basement block comprising the

250 Kemum Formation. Only one well reviewed by this study contained Silurian material,
251 no new analyses of outcrop samples of this age were undertaken in this study.

252 Water depths greater than 100m are interpreted based on the presence of
253 graptolites, typical of Paleozoic deep-water settings, found within the Kemum
254 Formation. This formation is described to contain sedimentary structures typical of
255 distal turbidites and the Aisasjur Formation, which outcrops at the western extent of
256 the Kemum basement block, is reported to comprise proximal turbidite deposits
257 (Pieters et al., 1983). This suggests the presence of localised north-east directed
258 bathymetric gradient and transport direction for turbiditic material in the central Bird's
259 Head (Fig. 6).

260 A broad south-easterly shallowing trend towards the Bird's Body is interpreted (Fig.
261 6). This based on the presence of the Modio Dolomite to the east of the Bird's Neck
262 and encountered within the **Cross Catalina-1** well farther to the east in the Bird's
263 Body (Fig. 6). The Modio Dolomite is interpreted by this study to have a shallow-
264 water carbonate-rich protolith, relative to the deeper water sediments to the north-
265 west.

266 4.3 Carboniferous

267 Palaeogeographic reconstructions of the Carboniferous are based on published
268 descriptions of formations of this age and review of two wells. No new analyses of
269 outcrop samples were conducted by this study.

270 Conglomerates, red beds and coal seams observed within the Aimau, Ainim and
271 Aiduna Formations of the Bird's Head and Neck suggest a terrestrial depositional
272 setting during the Carboniferous (Fig. 7; Pieters et al., 1983). This is supported by

273 the presence of plant-bearing terrestrial sediments reported from the Klalin-3 and
274 Puragi-1 wells.

275 Although the Aifat Mudstone is reported as marine (Pieters et al., 1983), the
276 deposition of this unit may have occurred during the early Carboniferous as the
277 previous period of Silurian high relative sea-level was waning (Fig. 5). Consequently,
278 a widespread terrestrial palaeodepositional setting is interpreted across the region
279 (Fig. 7).

280 4.4 Permian

281 The Permian palaeogeography interpreted by this study is based entirely on
282 published lithological descriptions and review of 23 on- and offshore wells. Of these
283 wells, 13 are interpreted to contain shallow water sediments based on occurrences
284 of delta front material and shallow water limestones. Ten wells are interpreted to
285 contain terrestrial deposits comprising combinations of red beds, coals, plants and
286 freshwater palynomorphs.

287 Permian deposits of western New Guinea are distributed within a narrow terrestrial
288 zone, extending across the central Bird's Head in the north, south into the Bird's
289 Neck and Body (Fig. 8). This terrestrial zone is surrounded by shallow water units,
290 interpreted to have been deposited in water depths no greater than 20m (Fig. 8).

291 The northern boundary of the terrestrial zone is drawn from the extent of outcrops of
292 the Aimau, Anim and Aiduna Formations across the Bird's Head and Neck. The
293 southern extent of the terrestrial zone is delineated by well data. No deep-water Aifat
294 mudstone is mapped with the rest of the Aifam Group in Figure 8 as it is interpreted
295 to be older than Permian.

296 4.5 Triassic

297 Reconstructions of palaeodepositional environments of Triassic rocks within western
298 New Guinea are based on the distribution of the Tipuma Formation data from 13
299 wells from the Bird's Head and island of Seram (Fig. 9).

300 The age of the Tipuma Formation is reported as no older than Late Triassic
301 (Gunawan et al., 2012) based on detrital zircon ages and is described to have been
302 deposited within an arid continental setting comprising unfossiliferous red-bed
303 sequences (Visser and Hermes, 1962; Pieters et al., 1983). This is supported by the
304 presence of oxidised sediments and continentally derived palynomorphs observed
305 within many of the seven wells interpreted to contain terrestrial deposits (Fig. 9). A
306 further six wells contain paralic and/or supralittoral sediments interpreted here to
307 represent shallow water depths, deposited in less than 20m water depth (Fig. 9).

308

309 Triassic continental deposits are widespread across much of western New Guinea
310 and Seram (Fig. 9). The Bird's Head is described to have remained in its present
311 position relative to Australia since the Triassic (Gunawan et al., 2012) and these
312 terrestrial deposits may extend farther south as part of the northern promontory of
313 the Australian continent, known as the 'Sula Spur'.

314

315 4.6 Early Jurassic

316 Early Jurassic data points are scarce within this study, with only two wells from the
317 Bird's Head and Body containing material of this age (Fig. 10). These wells contain
318 terrestrial sandstones of the Tipuma Formation, which continued to be deposited
319 until the Early Jurassic (Visser and Hermes, 1962; Pieters et al., 1983; Gunawan et
320 al., 2012). Consequently, a narrow zone of solely terrestrial deposits is interpreted to

321 extend from the Bird's Head, into the Neck and Body (Fig. 10), and possibly farther
322 into Australia as part of the Sula Spur.

323 4.7 Middle Jurassic

324 Across western New Guinea, a period of Late Triassic to Early Jurassic terrestrial
325 deposition, lasting at least 28 My, was succeeded deeper water sedimentation
326 during a transgressive event in the Middle Jurassic (Pieters et al., 1990; Lunt and
327 Djaafar, 1991; Gunawan et al., 2012; Figs. 5, 11). This is supported by review of 25
328 wells containing Middle Jurassic strata and material from eight outcrop locations.

329

330 It is interpreted that by the Middle Jurassic, relative sea-level had increased so that
331 much of the Sula Spur was submerged, reducing the once continuous peninsula to
332 an archipelago of isolated landmasses (Fig. 11). Two such landmasses were
333 separated by a narrow seaway with water depths between 50 and 100m (Fig. 11).

334 Terrestrial deposits are interpreted within six wells in the central Bird's Head and
335 southern Bird's Neck based on the presence of continentally derived palynomorphs.

336 A deltaic system is interpreted to the west of the northern landmass due to the
337 presence of fluvio-deltaic sediments reported within the CS-1X well (Fig. 11). These
338 landmasses are flanked by shallow seas of water depths no greater than 20m,
339 described from 18 wells. Water depths in excess of 50m are delineated by outcrops
340 of the Kopai Formation (Fig. 11).

341

342 The Kopai Formation is described to comprise deep-water black shales and
343 limestones (Pieters et al., 1983). Close to the village of Wendesi, Kopai Formation
344 black shales contain a common '*Macrocephalites*' ammonite assemblage. This
345 assemblage includes typical North Gondwanan species including *Macrocephalites*

346 *keeuwensis*, *Sphaeroceras boehmi* and *Holcophylloceras indicum* (Fig. 12). This
347 'Macrocephalites' ammonite assemblage is assigned a Bathonian-Callovian age
348 (Westermann & Callomon, 1988; Westermann, 1992; Westermann, 2000; van
349 Gorsel, 2012) and were deposited within a distal, deep, open marine setting (van
350 Gorsel, 2012).

351 The Middle Jurassic Tamrau Formation is described to comprise ammonites,
352 bivalves, and later planktonic foraminifera (Pieters et al., 1983) indicating a relatively
353 deep marine depositional environment. However, the Tamrau block is thought to be
354 allochthonous and translated to its current position along the Sorong Fault Zone
355 since the Pliocene.

356 4.8 Late Jurassic

357 Palaeogeographic reconstructions of this time interval are based on review of 26
358 wells containing Late Jurassic material and the distribution of the Kopai, Tamrau and
359 Woniwogi Formations of the Bird's Head, and Demu and Lelinta Formations of
360 Misool island. No outcrop samples were collected or examined of Late Jurassic age.

361 Continued regional transgression into the Late Jurassic (Fig. 5) saw the seaway
362 between the two landmasses of the former Sula Spur attain water depths in excess
363 of 100m (Fig. 13). The deltaic system to the west of the northern landmass is
364 interpreted to persist into the Late Jurassic due to the presence of sediments
365 reported within the CS-1X well (Fig. 13).

366 The Woniwogi, Demu and Lelinta Formations are interpreted to be deep-water
367 marine deposits, similar to the Kopai and Tamrau, based on the presence of
368 glauconitic and argillaceous, fine-grained, distal sediments (Pieters et al., 1983) and

369 bathyal agglutinated foraminifera such as *Glomospira* spp, and *Trochammina* spp.
370 within some wells (Murray, 2006).

371 4.9 Early Cretaceous

372 Only 10 of the reviewed wells contained material interpreted to be Early Cretaceous
373 in age, no outcrop samples were collected from this time interval. In addition to the
374 deep-water Kopai, Tamrau, Woniwogi, Demu and Lelinta Formations, the
375 widespread Early Cretaceous Piniya Mudstone is also interpreted to be a deep
376 marine deposit that comprises thinly bedded glauconitic black mudstones and muddy
377 siltstones (Pieters et al., 1983).

378 Due to the distribution of the Piniya Mudstone across the central Bird's Head, it is
379 interpreted that the northern remnant landmass of the Sula Spur was submerged at
380 this time beneath water depths in excess of 100m (Fig. 14). This is supported by the
381 presence ammonites and belemnites within the Kembelangan-1 well (Visser and
382 Hermes, 1962) and carinate Globotruncanid planktonic foraminifera, such as
383 *Praeglobotruncana* spp., *Paraglobotruncana* spp. and *Rotalipora* spp., in the
384 Kembelangan-1 and Noordwest-1 wells.

385 A bathymetric gradient shallows towards the south-west where water depths
386 between 50m and 100m are interpreted (Fig. 14). This is based on the presence of
387 shelfal agglutinated and calcareous benthic foraminifera, such as *Lenticulina* spp., in
388 the Onin East-1 well and sediments dominated by globular planktonic foraminifera
389 including *Hedbergella* spp., *Heterohelix* spp. and *Ticinella* spp., and lack of carinate
390 foraminifera, within the Kola-1 well. A small area to the south of the Bird's Body
391 remained subaerially exposed based on shallow water sandstones encountered in
392 the Cross Catalina-1 well.

393 Although the Woniwogi Formation is assigned a Late Jurassic to Early Cretaceous
394 age (Pieters et al., 1983), the planktonic foraminifera listed above (recorded from the
395 Woniwogi Formation in the Kembelangan-1, Noordwest-1 and Kola-1 wells) indicate
396 a restricted late Early Cretaceous, Aptian-Albian, age.

397 4.10 Late Cretaceous

398 Relative sea-level rise reached its peak during the Late Cretaceous (Fig. 5) where
399 water depths in excess of 100m are interpreted across the whole of western New
400 Guinea (Fig. 15). This is evident from data reviewed from 40 wells and six outcrop
401 samples, together with the distribution of Late Cretaceous deep-water sediments of
402 the Tamrau and Jass Formations, Piniya Mudstone, Amiri Sandstone of New Guinea
403 and pelitic rocks of the Korido Metamorphics of the island of Supiori (Fig. 15). Late
404 Cretaceous shallow-water Ekmai sandstones are interpreted to have been deposited
405 farther afield and brought into the Bird's Neck area through shortening in the
406 Lengguru Fold and Thrust Belt. The 'in situ' facies in the Bird's Neck is interpreted to
407 be represented by the deep marine Piniya Mudstone, following the trend for
408 increasing sea-level initiating in early Jurassic.

409 Many of the 40 wells contain diagnostic deep-water taxa, dominated by carinate
410 Globotruncanid planktonic foraminifera including, but not exclusively, *Abathomphalus*
411 *mayaroensis*, *Dicarinella* spp., *Gansserina gansseri*, *Globotruncana aegyptiaca*,
412 *Globotruncana arca*, *Globotruncana linneiana*, *Globotruncana ventricosa*,
413 *Globotruncanita* spp., *Globotruncanita stuartiformis*, *Helvetoglobotruncana helvetica*,
414 *Marginotruncana* spp., *Rosita* spp., *Rosita fornicata*, *Rotalipora* spp.,
415 *Rugoglobotruncana* spp., *Whiteinella* spp., *Whiteinella archeocretacea*, and globular
416 planktonic foraminifera including *Heterohelix* spp., *Pseudoguembelina* spp. and
417 *Racemiguembelina fructifera*. Where these carinate planktonic foraminifera occur in

418 abundance, this may indicate water depths in excess of 300m and an upper bathyal
419 depositional setting.

420 Campanian to Maastrichtian age sediments were collected from the Imskin
421 Limestone to the south-east of the Bird's Head (Fig. 15). Six samples contain deep-
422 water taxa, indicative of outer neritic to lower bathyal water depths in excess of
423 100m, including *Abathomphalus mayaroensis*, *Contusotruncana fornicata*, *C.*
424 *plummerae*, *Gansserina gansseri*, *Globotruncana arca*, *Globotruncana linneiana*,
425 *Globotruncanita conica*, *Gta. stuarti*, *Rugotruncana subcircumnodifer* and
426 *Heterohelix* spp (Fig. 16).

427

428 4.11 Paleocene

429 Following the Late Cretaceous relative sea-level high, water levels receded during
430 the Paleocene (Fig. 5) leaving shallower water areas around the southern Bird's
431 Head, Neck and Body (Fig. 17). This is based on review of 34 wells and examination
432 of five outcrop samples collected from the Imskin Limestone. The distribution of
433 shallow water areas up to 20m water depth is delineated by the distribution of the
434 Waripi Formation in outcrop, and encountered in wells particularly in the southern
435 Bird's Body (Fig. 17). The Waripi Formation is interpreted to comprise a shallow-
436 water limestone containing abundant oolites, miliolids and bryozoa (Visser and
437 Hermes, 1962; Brash et al., 1991). Farther north, particularly within the Bintuni basin,
438 deeper waters in excess of 100m are encountered in many wells recording turbiditic
439 material and carbonate mudstones comprising carinate and globular foraminifera
440 including *Morozovella* spp., *M. acuta*, *M. aequa*, *M. angulata*, *M. edgari*, *M.*
441 *inconstans*, *M. pseudobulloides*, *M. velascoensis*, *Acarinina* spp., *Eugubina* spp.,
442 *Globanomalina* spp. and *Subbotina* spp.

443

444 Five samples collected from the Imskin Limestone near the island of Rumberpon
445 were dated to be Paleocene age. All samples are interpreted to have been deposited
446 in an outer neritic to lower bathyal setting where water depths exceed 100m (Fig.
447 17). These samples contain a planktonic foraminiferal assemblage comprising
448 globular and carinate morphologies including *Acarinina coalingensis*, *A. primitiva*,
449 *Globanomalina imitata*, *G. ovalis*, *Morozovella aequa*, *M. angulata*, *M.*
450 *conicotruncata*, *Subbotina* spp. and *Turbeogloborotalia compressa*.

451

452 4.12 Early Eocene

453 Relative sea-level fall continued into the Early Eocene (Fig. 5) and more shallow
454 water areas developed within the central Bird's Head (Fig. 18). This is supported
455 from review of 25 wells, examination of nine outcrop samples and distribution of the
456 Faumai Limestone (Fig. 18).

457

458 The Faumai Limestone is described to contain shallow water carbonate bank and
459 shoal deposits and reefal facies (Pieters et al., 1983). This is supported by well data
460 where shallow water areas up to 20m in depth are interpreted north of the Bintuni
461 basin in southern Bird's Neck and Body based on the presence of alveolinids
462 including *Lacazinella* spp. and *Fasciolites* spp. Moderate water depths between 20m
463 and 50m are interpreted from the Faumai Limestone of several wells and outcrop
464 samples that contain alveolinids as well as abundant large, flat, rotaliine foraminifera
465 such as *Assilina* spp., *Cycloclypeus* spp., *Discocyclina* spp. and *Operculina* spp.
466 Pieters et al. (1983) date the Faumai Limestone as Middle Eocene to Oligocene in
467 age, however based on the presence of these alveolinids including *Alveolina*

468 *globosa*, *A. laxa* and *A. subpyrenaica*, and larger benthics including *Asterocyclina*
469 spp., *Discocyclina ranikotensis* and *Cuvillierina* spp. (Fig. 19), we interpret the
470 Faunai Limestone to be at least as old as Early Eocene, Ypresian, correlating to
471 planktonic foraminiferal zone E1 and Indo-Pacific letter stage 'Ta2' (Fig. 2).

472

473 Deeper water areas are interpreted to persist in the wells of the Bintuni basin, from
474 outcrop samples collected close to the island of Rumberpon and the Wandaman
475 Peninsula on the west coast of Cenderawasih Bay and in offshore areas west of
476 New Guinea (Fig. 18). The Bintuni wells contain mixtures of Early Eocene globular
477 and carinate planktonic foraminifera including *Morozovella* spp., *M. aragonensis*, *M.*
478 *formosa*, *M. quetra*, *M. subbotinae*, *Acarinina* spp., *Acarinina nitida* and *Subbotina*
479 spp. Rocks collected from the Imskin Limestone and Wandaman Peninsula also
480 suggest water depths greater than 100m (Fig. 18). Samples collected from these
481 localities contain the planktonic foraminifera *Acarinina* spp., *Acarinina bulbrooki*, *A.*
482 *decepta*, *Globigerina lozanoi*, *Globigerinatheka* spp., *Morozovella formosa*, *M.*
483 *lensiformis*, *M. subbotinae* and *Subbotina* spp (Fig. 19).

484

485 4.13 Middle - Late Eocene

486 The lowest Paleogene relative sea-level occurred across much of western New
487 Guinea during the Middle to Late Eocene (Fig. 5). Shallow water areas were
488 prevalent across the central Bird's Head and Seram, and extended throughout the
489 southern Bird's Neck and Body (Fig. 20). This is supported from review of 39 wells,
490 examination of 13 outcrop samples and distribution of the oldest units of the NGLG
491 observed to contain Middle to Late Eocene aged microfaunal assemblages (Fig. 20).

492

493 Well data from the offshore Salawati and Bintuni basin areas, Arafura Sea, and
494 onshore wells indicate the presence of shallow waters no greater than 20m depth
495 punctuated by isolated reefal build-ups across most of the central Bird's Head (Fig.
496 20). This is based primarily on the presence of shallow water and reef loving taxa
497 such as *Alveolina* spp., *Fasciolites* spp., *Lacazinella wichmanni*, *Nummulites* spp.,
498 *Nummulites djodjarkartae*, *Pararotalia* spp. and corals observed in wells **ASA-1X**
499 **(Darman, 2000)**, **Aum-1**, **Boka-1X**, **Merak Emas-1**, **Rawarra-1 (Decker, 2009)**, **Sago-**
500 **1**, **Sebyar-1** and **TBE-1X**. Bathymetric gradients away from the shallow water
501 platforms drop to depths approaching 50m (Fig. 20) where large flat rotaliines
502 including *Assilina* spp., *Discocyclusina* spp., *Heterostegina* spp., *Operculina* spp. and
503 assemblages of small calcareous benthic foraminifera typical of shelf settings are
504 found in wells **Kamakawala-1**, **Makiri-1D**, **Tarof-2** and **Wos-1**. Deep water facies are
505 interpreted in the **Onin East-1** well based on the presence of *Acarinina* spp.,
506 *Globigerinatheka* spp. and *Morozovella* spp.

507

508 Interpretations from well data are supported by outcrop evidence from the western
509 Cenderawasih Bay. Close to the village of Ransiki, shallow water facies include
510 grainstones containing large *Alveolina elliptica* and *Nummulites gizehensis* within
511 samples of the Faumai Limestone (Fig. 21). Farther to the south-east of Ransiki,
512 samples contain large flat rotaliines including *Assilina exponens*, *Asterocyclusina* sp.
513 and *Discocyclusina sella* indicative of moderate water depths. Water depths between
514 50m and 100m are interpreted close to the island of Rumberpon (Fig. 20), where
515 rocks of the Imskin Limestone contain the planktonic foraminifera *Acarinina*
516 *intermedia*, *Globigerina tripartita*, *Porticulasphaera mexicana* and *Subbotina* spp.
517 Rocks of the Imskin Limestone and Wandaman Peninsula indicate outer neritic water

518 depths in excess of 100m surrounding the Wandaman peninsula. Samples here
519 contain a mixture of globular planktonic foraminifera including *Acarinina decepta*, *A.*
520 *pentacamerata*, *A. primitiva*, *A. pseudotopilensis*, *Globigerinatheka* sp., *Subbotina*
521 *eocaenica* and carinate forms including *Morozovella aragonensis* and *M. crassata*.
522

523 The oldest foraminifera observed on the islands of Biak and Supiori are *Pellatispira*
524 sp., an exclusively Late Eocene, Priabonian, aged genus indicative of Indo-Pacific
525 'letter stage' Tb (Adams, 1970; Figs. 2 & 21). These larger benthic foraminifera are
526 found reworked within clasts of Auwewa Formation material within the Batu Ujang
527 Conglomerate outcropping around Wafordori Bay on the north coast of Supiori.
528 Although reworked, *Pellatispira* sp. signify moderate water depths up to several 10's
529 of metres within the vicinity of Supiori. This taxon is also observed within the
530 Auwewa Formation encountered in wells H-1, Muwar-1, O-1 and R-1 in eastern
531 Cenderawasih Bay and Mamberamo region.

532

533 4.14 Oligocene

534 Relative sea-level rose for a short while across western New Guinea during the
535 Oligocene (Fig. 5). Palaeogeographic reconstructions of this time interval are based
536 on review of 25 wells, examination of six outcrop samples and distribution of the
537 Sirga Formation (Fig. 22).

538

539 Small islands of terrestrially derived Oligocene sediments are interpreted in the
540 Bird's Neck from wells Suga-1 and ASB-1X (Fig. 22). These are surrounded by
541 shallow bodies of water with occasional reefal build-ups interpreted based on the
542 presence of *Austrotrillina* spp. and *Nummulites* spp recorded from several wells,

543 including TBE-1X (Fig. 22). Water depths up to 50m are extensive around the
544 southern Bird's Head and Neck (Fig. 22) are denoted by the presence of larger
545 benthic foraminifera including *Cycloclypeus* spp., *Heterostegina borneensis*,
546 *Operculina* spp. and *Pararotalia metacapensis*. Deeper waters are interpreted in the
547 Salawati basin region, Seram Sea and much of the central Bird's Head (Fig. 22)
548 where Oligocene aged rocks, including those of the Sirga Formation, are dominated
549 by intermediate water depth taxa such as *Catapsydrax* spp., *Globigerina*
550 *ampliapertura*, *Globoturborotalita ouachitaensis*, *Paragloborotalia opima* recorded
551 from Klalin-1, Merak Emas-1 and Siganoi-1.

552

553 Six samples of Early and Late Oligocene age were collected from the west coast of
554 Cenderawasih Bay (Fig. 22). Shallow water reef front facies, representing water
555 depths no greater than 10m, are found near the island of Rumberpon where samples
556 contain specimens of *Neorotalia* sp. and one of the last species of *Nummulites*, the
557 reticulate *N. fichteli* (BouDagher-Fadel, 2008).

558

559 Late Oligocene rocks are observed in sedimentary lenses of the Arfak Volcanics of
560 the eastern Bird's Head and Auwewa Formation on Supiori (Fig. 22). These samples
561 consist of planktonic foraminiferal packstones and wackestones indicating outer
562 slope depths between 50m and 100m. Planktonic foraminifera of 'intermediate-
563 water' depths consist of globular morphologies including *Globigerina gortanii*,
564 *Globigerina praebulloides*, *Globigerinoides primordius* and *Globoquadrina binaiensis*.

565

566 4.15 Early Miocene

567 The Early Miocene saw the presence of widespread shallow water carbonate
568 platforms across western New Guinea and Cenderawasih Bay, with maximum water
569 depths no greater than 50m (Fig. 23). This is supported from review of 50 wells and
570 examination of 37 outcrop samples. Early Miocene aged units of the NGLG including
571 the Kais, Koor and Maruni Limestones of New Guinea, the Wurui Limestone of
572 Yapen, and Wainukendi and Wafordori Formations of Biak and Supiori are described
573 to comprise predominantly shallow water to reefal carbonates (Visser and Hermes,
574 1962; Pieters et al., 1983). These units were mapped without distinction between
575 shallow and relatively deeper water facies; therefore the distribution of these
576 formations is used only to interpret water depths no greater than 50m to
577 accommodate potential heterogeneity within the NGLG.

578

579 A broad platform populated by reefal build-ups extending from the western Bird's
580 Head to the southern Bird's Neck and Body (Fig. 23). This is interpreted from 41
581 wells comprising packstones, grainstones and reefal rudstones and floatstones that
582 contain shallow water taxa including *Alveolinella praequoyi*, *Amphistegina* spp.,
583 *Austrotrillina* spp., *Borelis* spp., *Flosculinella* spp., *Lepidocyclina* spp., miliolids,
584 *Miogypsina* spp., *Miogypsinoides* spp., *Spiroclypeus* spp. and other organisms
585 including sponges, coral, echinoids and bivalves. Further shallow water platforms
586 are interpreted to have occurred across Cenderawasih Bay, encompassing the
587 islands of Yapen, Biak and Supiori (Fig. 23). These platforms sit atop an extensive
588 body of water no greater than 50m (Fig. 23) based on the presence of the larger
589 benthic foraminifera *Operculina* spp., *Heterostegina* spp. and *Cycloclypeus* spp.
590 Rare deeper water sediments were encountered in the Oseil-1 of Seram contained

591 the globular planktonic foraminifera *Globigerinoides* spp, *Globigerina* spp. and
592 *Catapsydrax* spp.

593

594 In outcrop, many reefal carbonates are observed at the base of the Kais and Maruni
595 Limestones of the mainland and Wainukendi Formation of Biak and Supiori. These
596 reefs are mapped isolated patch reefs in Figure 23, although their lateral extent is
597 unknown. Reefal carbonates and those deposited in moderate water depths were
598 observed to contain an abundant and diverse fossil assemblage, predominantly
599 comprising larger benthic foraminifera including: *Eulepidina badjirraensis*,
600 *Lepidocyclina brouweri*, *L. isolepidinoides*, *L. nephrolepidinoides*, *L. oneatensis*, *L.*
601 *stratifera*, *L. sumatrensis*, *Heterostegina borneensis*, *Miogypsina intermedia*, *M.*
602 *kotoi*, *M. tani*, *Miogypsinoidea bantamensis*, *Mdes. dehaarti*, *Miogypsinoidea*
603 *primitiva*, *Miolepidocyclina*, *Operculina* sp. and *Spiroclypeus tidoenganensis* (Fig.
604 24).

605

606 4.16 Middle Miocene

607 A second regional transgressive event is interpreted to have initiated in the
608 Burdigalian (Gold et al., in review) so that by the Middle Miocene much of western
609 New Guinea was submerged in water up to 100m depth (Fig. 25). Evidence for a rise
610 in relative sea-level can be found in deep water facies of the Napisendi Formation
611 and Sumboi Marl of the islands of Cenderawasih Bay, and in drowning successions
612 at the top Maruni and Kais Limestone (Gold et al., in review).

613 Early Miocene shallow water carbonate platforms were replaced by more moderate
614 water depths in the Salawati and Bintuni basins, and areas south of the Bird's Head
615 while backstepping to shallow water regions to the north-east of the island of Supiori

616 (Fig. 25). Taxa indicative of moderate water depths, including *Cycloclypeus* spp.,
617 *Operculina* spp., and *Pseudorotalia* spp., are prevalent in 18 wells distributed across
618 western New Guinea (Fig. 25). Isolated carbonate platforms and occasional pinnacle
619 reefs are recorded in the main basins of the Bird's Head which contain the shallow
620 water taxa *Alveolinella quoyi*, *Flosculinella bontangensis*, *Lepidocyclina* spp.,
621 *Marginopora vertebralis*, *Miogypsina* spp. as well as corals, red algae, bivalves and
622 echinoids. Deeper water areas are interpreted from the presence of planktonic
623 foraminiferal assemblages including the taxa: *Orbulina universa*, *Globigerina druryi*,
624 *Globigerinoides subquadratus*, *Globigerinoides diminutus*, *Globigerinoides*
625 *bisphaericus*, *Praeorbulina glomerosa*, *Praeorbulina transitoria*, *Paragloborotalia*
626 *siakensis*, *Globorotalia fohsi*.

627

628 Shallow water deposits collected from outcrop include soritid foraminifera such as
629 *Marginopora vertebralis*, and miliolids including *Quinqueloculina* spp. and
630 *Alveolinella quoyi* observed in the Koor Formation situated in the Tosem Mountains
631 in the northern 'cap' of the Bird's Head and interbedded within the Napisendi
632 Formation on Biak. An isolated reef is interpreted near the island of Rumberpon at
633 this time (Fig. 25), where samples contain reef-loving organisms such as
634 miogypsinid and lepidocyclinid larger benthic foraminifera.

635

636 Samples from the Kais and Maruni Limestones of the Bird's Head and the Wafordori
637 Formation on Biak contain large flat rotaliine foraminifera including *Katacycloclypeus*
638 *annulatus* and *Cycloclypeus carpenteri*, lepidocyclinids including *Lepidocyclina*
639 *brouweri*, *L. ferreroi*, *L. omphalus*, *L. verbeeki*, miogypsinids including

640 *Miogypsinooides indica*, *Miogypsina cushmani*, *M. intermedia*, *M. kotoi*, *M. regularia*
641 (Fig. 26).

642

643 Deep water deposits occur in the upper parts of the Kais and Maruni Limestones and
644 Napisendi Formation, extending south to the central Bird's Head and Cenderawasih
645 Bay (Fig. 25). These samples contain abundant globular planktonic foraminifera that
646 indicate intermediate water depths between 50m and 100m. Examples include
647 *Orbulina suturalis*, *O. universa*, and many species of *Globigerinoides* including *G.*
648 *quadrilobatus*, and *G. trilobus*, amongst others and rare *Globorotalia* spp. (Fig. 26).

649

650 4.17 Late Miocene

651 Relative sea-level continued to rise so that water depths greater than 50m were
652 widespread across much of the present day western New Guinea during the Late
653 Miocene (Figs. 5 & 27). Deep water facies rocks are represented by the Befoor and
654 Klasafet Formations of the Bird's Head and Neck, encountered in 67 of the reviewed
655 wells and in 24 outcrop samples (Fig. 27).

656

657 Evidence for the prevalence of water depths between 50m and 100m in the eastern
658 Bird's Head and islands to the north of Cenderawasih Bay come from the abundance
659 of 'intermediate-water' species including *Candeina nitida* and *Orbulina suturalis* (Bé,
660 1977) found in outcrop samples. Farther south, in samples collected close to the
661 island of Rumberpon (Fig. 27), water depths in excess of 100m are interpreted due
662 to abundance of carinate planktonic foraminifera including *Globorotalia plesiotumida*,
663 *Truncorotalia ronda* and the thick-walled globular planktonics *Sphaeroidinellopsis*
664 *subdehiscens* and *Globoquadrina dehiscens*. These water depths are interpreted

665 from wells in the Salawati and Bintuni basins, and Arafura Sea, based on the
666 presence of thick-walled and carinate planktonic foraminifera including those
667 mentioned above and *Dentoglobigerina baroemoensis*, *Globorotalia merotumida*,
668 *Neogloboquadrina acostaensis*, *Neogloboquadrina humerosa* and
669 *Sphaeroidinellopsis* spp.

670

671 4.18 Early Pliocene

672 Open marine settings remained the dominant depositional environment across
673 western New Guinea during the Early Pliocene (Fig. 28). Deep water facies are
674 recorded from the Klasaman, Opmorai and Befoor Formations of the Bird's Head,
675 and Wardo, Korem and Kurudu Formations of the islands of Cenderawasih Bay (Fig.
676 28). Water depths in excess of 50m are recorded from 59 wells across western New
677 Guinea (Fig. 28) that contain microfossils assemblages dominated by globular and
678 carinate planktonic foraminifera including *Globigerina* spp., *Globigerinoides* spp.,
679 *Globorotalia* spp., *Neogloboquadrina* spp., *Sphaeroidinella* spp. and
680 *Sphaeroidinellopsis* spp.

681

682 Relatively shallower water facies are recorded from 9 wells south and west of the
683 Bird's Head and in the central Bird's Body (Fig. 28). This is supported by the
684 presence of shallow water facies including grainstones, coral floatstones and back-
685 reef lagoonal wackestones that contain the taxa *Ammonia* spp., *Amphistegina*
686 *lessonii*, *Calcarina spengleri*, *Heterostegina* spp., *Marginopora* spp., *Neorotalia*
687 *calcar*, *Pararotalia* spp., *Peneroplis* spp., *Pseudorotalia* spp. and miliolids.

688

689 Outcrop samples collected from the Befoor and Klasaman Formations in the eastern
690 Bird's Head were observed to contain abundant globular planktonic foraminifera
691 including many species of *Globigerinoides* spp., *Neogloboquadrina* spp., *Pulleniatina*
692 spp., *Sphaeroidinella* spp. and *Sphaeroidinellopsis* spp., as well as *Orbulina*
693 *universa*. Carinate planktonic foraminifera such as species of *Globorotalia* spp. are
694 interpreted to have been occasionally washed in to this environment and large flat
695 benthic foraminifera such as *Operculina* spp. are washed down slope. To the north-
696 east of the Bird's Head, evidence for shallower reefal settings are observed with reef
697 front facies rocks of the Wai Limestone containing *Calcarina spengleri*, *Amphistegina*
698 spp. and abundant rodophyte red algae situated in front of back-reef facies units
699 (Fig. 28). Shallow water facies, interpreted as back-reef lagoons, to the east of the
700 Bird's Head (Fig. 28) contain soritid foraminifera including *Marginopora vertebralis*,
701 small rotaliids including *Quasirootalia guamensis* as well as delicate corals and the
702 dasycladacean green alga, *Halimeda*.

703

704 On the islands of Biak and Supiori, a small bathymetric high is interpreted to pass
705 quickly from inner slope sediments into outer neritic settings indicating the presence
706 of steeply inclined slopes around the high (Fig. 28). Outer neritic sediments
707 representing water depths in excess of 100m occur towards the Biak basin to the
708 south-west. These sediments contain common carinate planktonic foraminifera
709 including *Globorotalia conoidea*, *G. margaritae*, *G. menardii*, *G. miocenica*, *G.*
710 *tumida*, *G. sphericomiozea*, *Truncorotalia crassula* and thick walled globular
711 planktonic foraminifera *Sphaeroidinellopsis seminulina*. Carinate planktonic
712 foraminifera are indicative of water depths in excess of 100m were observed in deep
713 water facies of the Korem and Wardo Formations.

714

715 4.19 Late Pliocene

716 Regression initiating in western New Guinea towards the end of the Early Pliocene
717 (Fig. 5) resulted in more extensive and frequent shallow water areas interpreted
718 across the region by the Late Pliocene (Fig. 29). This is supported by review of 64
719 wells and 29 outcrop samples. Deep water areas are interpreted based on the
720 presence of globular and carinate planktonic foraminifera including *Globigerina* spp.,
721 *Globigerinoides* spp., *Globorotalia* spp., *Neogloboquadrina* spp., *Sphaeroidinella*
722 spp. and *Sphaeroidinellopsis* spp. The distribution of relatively shallower areas are
723 interpreted based on the presence of large flat rotaliines including *Cycloclypeus*,
724 *Heterostegina* spp., *Operculina* spp. and typical back reef or lagoonal taxa such as
725 soritid and miliolid foraminifera, coral, echinoids and bivalves.

726

727 4.20 Pleistocene

728

729 Early Pliocene relative sea-level fall continued into the Pleistocene and up to the
730 present day in western New Guinea (Fig. 5). Several areas of the Bird's Head, Neck
731 and Body were submerged beneath waters no greater than 50m. In the location of
732 the present day islands of north of Cenderawasih Bay carbonate platforms deposited
733 shallow water and reefal facies rocks of the coeval Mokmer and Manokwari
734 Formations (Fig. 30). At this time Cenderawasih Bay itself became a distinct deep
735 water feature filled by pelagic carbonates comprising planktonic foraminiferal
736 packstones. Localised areas were subaerially exposed close to the Salawati and
737 Bintuni basins (Fig. 30) as a precursor to the present day topography of the island of
738 New Guinea.

739

740 Only five samples were collected of Pleistocene age (Fig. 30). Four samples
741 representing the Mokmer Formation were located to the south-east of Biak and one
742 sample from the Manokwari Formation of the north-eastern Bird's Head (Fig. 30).
743 Palaeogeographic interpretations suggest a southwest directed deepening trend
744 across a broad carbonate platform no deeper than 50m in water into the much
745 deeper setting of Cenderawasih Bay (Fig. 30). The presence of a carbonate platform
746 attaining these moderate water depths is indicated by common occurrences of the
747 larger benthic foraminifera *Heterostegina* spp., and globular planktonic foraminifera
748 including *Pulleniatina obliquiloculata* and *Globigerinoides quadrilobatus*. Rocks
749 interpreted to have been deposited in reefal, shallow water settings up to 10m in
750 depth comprise grainstones that contain abundant encrusting rodophyte red algae
751 resilient to the brunt of high hydrodynamic energies. Behind this, quiet waters of the
752 former back-reef are situated to the east of the island and contain delicate bryozoa
753 and branching corals of the genera *Acropora* and *Porites*. Dasycladacean green
754 algae, such as *Halimeda*, are also common. The disintegration of algal needles may
755 contribute towards the large amount of micrite in wackestones deposited in this
756 setting.

757 **5. Conclusions**

758

759 Biostratigraphy of well data and outcrop samples reveals a reasonably conformable
760 sequence of sediments dated from the Silurian to present day. Two major
761 transgressive-regressive cycles in relative sea-level are identified within the region
762 (Fig. 5). Peaks in relative sea-level are interpreted to have occurred in the Late
763 Cretaceous and Late Miocene (Fig. 5), with the latter tentatively correlated to the
764 global Tor1 maximum flooding surface at 10.51 Ma where global sea-level was

765 approximately 80m higher than today (Snedden and Liu, 2010; Gold et al., in
766 review).

767

768 As the position of New Guinea position relative to Australia has not changed
769 considerably since the Triassic (Gunawan et al., 2012), it is interpreted that our
770 palaeogeographic reconstructions south of the Australia-Pacific suture from the
771 Triassic onwards are relatively robust. Confidence in the robustness of the
772 reconstructions using post-collisional stratigraphy of the region is also high.
773 However, displacements along major strike-slip fault systems such as the Sorong
774 Fault Zone, interpreted to have initiated in the Early Miocene (Visser and Hermes,
775 1962; Ali and Hall, 1995), may distort the reconstructions.

776 **Acknowledgments**

777 This work was supported by the Southeast Asia Research Group at Royal Holloway,
778 funded by a consortium of oil companies. We would like to thank our fieldwork
779 counterparts from the Institut Teknologi Bandung, John Decker, Phil Teas, Angus
780 Ferguson and the crew of the Shakti for assistance during fieldwork and staff
781 members at Royal Holloway, University of London, for enabling this study to take
782 place. In particular we would like to thank Robert Hall for continued mentoring,
783 guidance, helpful discussion and facilitating the progression of our understanding of
784 a geologically complex and exciting region of the world through his work with the
785 Southeast Asia Research Group.

786 **References**

787 Adams, C.G., 1965. The foraminifera and stratigraphy of the Melinau Limestone,
788 Sarawak, and its importance in Tertiary correlation. *Quarterly Journal of the*
789 *Geological Society*, 121(1-4), pp.283-338.

790 Adams, C.G. (1970) A reconsideration of the East Indian letter classification of the
791 Tertiary, *Bulletin of the British Museum (Natural History)*. *Geology*, 19, 87-137.

792 Ali, J. R. and Hall, R. 1995. Evolution of the boundary between the Philippine Sea
793 Plate and Australia: Palaeomagnetic evidence from eastern Indonesia.
794 *Tectonophysics*, **251 (1-4)**, 251-275

795 Baldwin, S. L., Fitzgerald, P. G. and Webb, L. E. 2012. Tectonics of the New Guinea
796 Region. *Annual Reviews from Earth and Planetary Science*, **40**, 495-520

797 **Baldwin and Ireland**

798 Bé, A. W. H. (1977) An ecological, zoogeographic and taxonomic review of Recent
799 planktonic foraminifera. In: *Oceanic micropalaeontology* (Ed. by A. T. S. Ramsey), 1-
800 100. Academic Press, London.

801 Beavington-Penney, S. J., and Racey, A., 2004. Ecology of extant nummulitids and
802 other larger benthic

803 Berggren, W.A. and Miller, K.G., 1988. Paleogene tropical planktonic foraminiferal
804 biostratigraphy and magnetobiochronology. *Micropaleontology*, pp.362-380.

805

806 Berggren W.A., Kent, D.V., Swisher, C.C., III, Aubry, M.-P., 1995. A revised
807 Cenozoic geochronology and chronostratigraphy. In: Berggren, W.A., Kent, D.V.,
808 Aubry, M.-P., Hardenbol, J. (Eds.), *Geochronology, Time Scales, and Stratigraphic*
809 *Correlation: Framework for an Historical Geology*. *SEPM Spec. Publ.*, 54:129-212.

810

811 Blow, W.H., 1979. *The cainozoic Globigerinida: a study of the morphology,*
812 *taxonomy, evolutionary relationships and the stratigraphical distribution of some*
813 *Globigerinida (mainly Globigerinacea). Text: P. 1/2: Sect. 1. Brill.*
814

815 Bock, Y., Prawirodirdjo, L., Genrich, J. F., Stevens, C. W., McCaffrey, R., Subarya,
816 C., Puntodewo, S. S. O. & Calais, E. (2003) Crustal motion in Indonesia from Global
817 Positioning System measurements. *Journal of Geophysical Research*, 108 (B8),
818 2367, ETG 3-1-21.

819 BouDagher- Fadel, M.K. (2015) *Biostratigraphic and geological significance of*
820 *planktonic foraminifera*. UCL Press, London.

821 BouDagher-Fadel, M. K. (2008) Evolution and geological significance of larger
822 benthic foraminifera. *Developments in palaeontology and stratigraphy*, 21. Elsevier,
823 Amsterdam.

824 Brash, R. A., Henage, L. F., Harahap, B. H., Moffat, D. T., & Tauer, R. W. (1991)
825 Stratigraphy and depositional history of the New Guinea limestone group, Lengguru,
826 Irian Jaya. *Proceedings Indonesian Petroleum Association 12th Annual Convention*,
827 67-84.

828 Charlton, T. R. 2010. The Pliocene-recent anticlockwise rotation of the Bird's Head,
829 the opening of the Aru trough – Cenderawasih bay sphenochasm, and the closure of
830 the Banda double arc. *Proceedings of the 34th Indonesian Petroleum Association*
831 *convention and exhibition*, IPA10-G-008

832 Cloos, M., Sapiie, B., van Ufford, A. Q., Weiland, R. J., Warren, P. Q. & McMahon, T.
833 P. (2005) Collisional delamination in New Guinea: The geotectonics of subducting
834 slab breakoff. *Geological Society of America Special Paper*, 400, 46pp.

835 **Davies – Review**

836 Gold, D., Burgess, P. M. and BouDagherFadel, M. K. Carbonate drowning
837 successions of the Bird's Head (in review.)

838 Gunawan, I., Hall, R. and Sevastjanova, I. 2012. Age, character and provenance of
839 the Tipuma Formation, West Papua: New insights from detrital zircon dating.
840 *Proceedings Indonesian Petroleum Association 36th Annual Convention*, IPA12-G-
841 027, 1-14

842 Gunawan, I., Hall, R., Augustsson, C. and Armstrong, R. 2014. Quartz from the
843 Tipuma Formation, West Papua: new insights from geochronology and
844 cathodoluminescence studies. *Proceedings of the Indonesian Petroleum Association*
845 *38th Annual Convention and Exhibition*, IPA14-G-303

846 Hall, R. (2012) Late Jurassic–Cenozoic reconstructions of the Indonesian region and
847 the Indian Ocean. *Tectonophysics*, 570-571, 1-41.

848 Hall, R. 2002. Cenozoic geological and plate tectonic evolution of SE Asia and the
849 SW Pacific: computer-based reconstructions, model and animations, *Journal of*
850 *Asian Earth Sciences*, 20, 353-431.

851 Hallock, P. AND Glenn, E.C. (1986) Larger foraminifera: a tool for
852 paleoenvironmental analysis of Cenozoic carbonate depositional facies. *Palaios*, 55-
853 64.

854 Hill, K. C. and Hall, R., 2003. Mesozoic-Cainozoic evolution of Australia's New
855 Guinea Margin in a west Pacific context. In: Hillis, R. and Müller, R. D. (Eds) Defining
856 Australia: The Australian Plate as part of Planet Earth. Geological Society of America
857 Special Paper/Geological Society of Australia Special Publication 372, 265-290.

858 Hill;

859 Jacques

860 Lunt, P., and Djaafar, R., 1991, Aspects of the stratigraphy of western Irian Jaya and
861 implications for the development of sandy facies. Proceedings, 20th Indonesian
862 Petroleum Association Annual Convention, p. 107–124.

863

864 Lunt, P., 2013. Foraminiferal micropalaeontology in SE Asia In: A.J. Bowden et al.
865 (eds.)
866 Landmarks in foraminiferal micropalaeontology: history and development, The
867 Micropalaeontological Society, Spec. Publ. 6, Geol. Soc. London, p. 193-206.

868

869 Martini, R., Zaninetti, L., Lathuilliere, B., Cirilli, S., Cornée, J.J. and Villeneuve, M.,
870 2004. Upper Triassic carbonate deposits of Seram (Indonesia): palaeogeographic
871 and geodynamic implications. *Palaeogeography, Palaeoclimatology, Palaeoecology*,
872 206(1), pp.75-102.

873

874 Masria, M., Ratman, N. and Suwitodirdjo. 1981. Geologi lembar Biak, Irian Jaya (The
875 geology of the Biak Quadrangle, Irian Jaya), Geological Research and Development
876 Centre, Indonesia, 10pp

877 Metcalfe, I., 2009, Late Palaeozoic and Mesozoic tectonic and palaeogeographical
878 evolution of SE Asia. In Buffetaut, E., Cuny, G., Loeuff, J.L., and Suteethorn, V.,
879 eds., Late Palaeozoic and Mesozoic ecosystems in SE Asia: London, Geological
880 Society of London Special Publication 315, p. 7–23.

881

882 Milsom, J., Masson, D., Nichols, G., Sikumbang, N., Dwiyanto, B., Parson, L. and
883 Kallagher, H., 1992. The Manokwari Trough and the western end of the New Guinea
884 Trench. *Tectonics* 11 (1), 145-153.

885 Murray, J.W., 2006. *Ecology and applications of benthic foraminifera*. Cambridge
886 University Press.

887

888 Pieters, P. E., Hakim, A. S. and Atmawinata, S. 1990. Geologi lembar Ransiki, Irian
889 Jaya (Geology of the Ransiki sheet area, Irian Jaya), Geological Research and
890 Development Centre, Indonesia

891 Pieters, P. E., Hartono, U. and Amri, C. 1989. Geologi lembar Mar, Irian Jaya
892 (Geology of the Mar sheet area, Irian Jaya), Geological Research and Development
893 Centre, Indonesia

894 Pieters, P. E., Pigram, C. J., Trail, D. S., Dow, D. B, Ratman, N. & Sukamto, R.
895 (1983) The stratigraphy of the western Irian Jaya. *Bulletin of the Geological
896 Research and Development Centre*, 8, 14-48.

897 **Pigram;**

898 Robinson, G. P., Ratman, N. and Pieters, P. E. 1990. Geology of the Manokwari
899 sheet area, Irian Jaya, Geological Survey of Indonesia, Directorate of Mineral
900 Resources, Geological Research and Development Centre, Bandung

901 Snedden, J.W. & Liu, C. (2010) A compilation of Phanerozoic sea-level change,
902 coastal onlaps and recommended sequence designations. *AAPG Search and*
903 *Discovery Article*, 40594.

904 Van Gorsel, J.T., 1988. Biostratigraphy in Indonesia: methods, pitfalls and new
905 directions. . Proceedings, Indonesian Petroleum Association Annual Convention
906

907 van Gorsel, J. T. 2012. Middle Jurassic Ammonites from the Cendrawasih Bay Coast
908 and North Lengguru Fold-Belt, West Papua: Implications of a 'forgotten' 1913 Paper,
909 *Berita Sedimentologi*, v. 23, p.35-41
910

911 Visser, W.A. & Hermes, J.J. (1962) *Koninklijk Nederlands Geologisch*
912 *Mijnbouwkundig genootschap Verhandelingen Geologische (Geological results of*
913 *the search for oil in Netherlands New Guinea)*. Nederlandsche Nieuw Guinee
914 Petroleum Maatschappij.

915 Wade, B. S., Pearson, P. N., Berggren, W. A., & Pälike, H. (2011) Review and
916 revision of Cenozoic tropical planktonic foraminiferal biostratigraphy and calibration
917 to the geomagnetic polarity and astronomical time scale. *Earth-Science Reviews*,
918 104,111–142.

919 Webb, M., White, L.T., 2016. Age and nature of Triassic magmatism in the Netoni
920 Intrusive
921 Complex, West Papua, Indonesia, *Journal of Asian Earth Sciences*

922

923 Westermann, G.E.G. and Callomon, J.H., 1988. The Macrocephalitinae and
924 associated Bathonian and early Callovian (Jurassic) ammonoids of the Sula islands
925 and New Guinea. *Palaeontographica A*, 203, p. 1-90.

926

927 Westermann, G.E.G., 1992. *Jurassic of the Circum-Pacific*. Cambridge University
928 Press

929 Westermann, G.E., 2000. Marine faunal realms of the Mesozoic: review and revision
930 under the new guidelines for biogeographic classification and nomenclature.

931 *Palaeogeography, Palaeoclimatology, Palaeoecology*, 163(1), pp.49-68.

932

933 Wilson, M. E. J. 2002. Cenozoic carbonates in Southeast Asia: implications for
934 equatorial carbonate development. *Sedimentary Geology*, 147, p295– 428

935

936 **Figure Captions**

937 Figure 1. Structural map of western New Guinea. Faults were drawn based on
938 features identified from ASTER digital elevation data, bathymetric multibeam and
939 seismic data of the Biak and Cenderawasih Bay basins provided by TGS, and those
940 encountered in the field. The offshore Manokwari Trough was drawn from GLORIA
941 sonar imagery (after Milsom *et al.*, 1992). Derived regional stresses are implied after
942 Bock *et al.* (2003), and vector of Pacific-Caroline plate motion plotted after Cloos *et*
943 *al.* (2005).

944

945 Figure 2. Stratigraphy of the north and eastern Bird's Head. Established from field
946 data of this study and modified from Masria et al. (1981); Pieters et al. (1989);
947 Robinson et al. (1990); Pieters et al. (1990); Brash et al. (1991).

948

949 Figure 3. Geological map of units encountered during this study. Distribution of
950 geological units based on original GRDC maps and fieldwork from this study
951 (Modified from Masria et al., 1981; Pieters et al., 1989; Robinson et al., 1990; Pieters
952 et al., 1990)

953

954 Figure 4. The bathymetric boundaries used in the palaeogeographic reconstructions
955 are derived from environmental preferences of foraminifera observed in this study.
956 Thick lines indicate environments in which foraminifera are abundant, thin lines
957 indicate environments in which they also occur infrequently. Environmental
958 preferences are based on field data and Bé (1977), Hallock and Glenn (1986), van
959 Gorsel (1988), Brash et al., 1991; BouDagher-Fadel (2008, 2015), Beavington-
960 Penney and Racey (2004), Lunt (2013).

961

962 Figure 5. Relative sea-level curve based on the palaeogeographic reconstructions of
963 an arbitrary data point in northern Bintuni Bay. Two main transgressive-regressive
964 cycles are interpreted with peak relative sea-level occurring during the Late
965 Cretaceous and Late Miocene.

966

967 Figure 6. Palaeogeographic reconstruction of western New Guinea during the
968 Silurian. Based on evidence from Silurian aged sediments encountered in 1 well and
969 distribution of the Kemum and Aisasjur Formations, and Modio Dolomite.

970

971 Figure 7. Palaeogeographic reconstruction of western New Guinea during the
972 Carboniferous. Based on evidence from Carboniferous aged sediments encountered
973 in 2 wells and distribution of Aifam Group sediments.

974

975 Figure 8. Palaeogeographic reconstruction of western New Guinea during the
976 Permian. Based on evidence from Permian aged sediments encountered in 24 wells
977 and distribution of Aifam Group sediments.

978

979 Figure 9. Palaeogeographic reconstruction of western New Guinea during the
980 Triassic. Based on evidence from Triassic aged sediments encountered in 13 wells
981 and distribution of the Tipuma Formation.

982

983 Figure 10. Palaeogeographic reconstruction of western New Guinea during the Early
984 Jurassic. Based on evidence from Early Jurassic aged sediments encountered in 2
985 wells and distribution of the Tipuma Formation.

986

987 Figure 11. Palaeogeographic reconstruction of western New Guinea during the
988 Middle Jurassic. Based on evidence from Middle Jurassic aged sediments
989 encountered in 25 wells, 8 outcrop samples and distribution of the Kopai and Tamrau
990 Formations.

991

992 Figure 12. Bathonian-Callovian aged ammonites collected from the Kopai Formation
993 close to the village of Wendesi. A) *Macrocephalites keeuwensis*, B) *Sphaeroceras*
994 *boehmi* and C) *Holcophylloceras indicum*

995

996 Figure 13. Palaeogeographic reconstruction of western New Guinea during the Late
997 Jurassic. Based on evidence from Late Jurassic aged sediments encountered in 26
998 wells and distribution of the Kopai, Tamrau, Woniwogi, Demu and Lelinta
999 Formations.

1000

1001 Figure 14. Palaeogeographic reconstruction of western New Guinea during the Early
1002 Cretaceous. Based on evidence from Early Cretaceous aged sediments encountered
1003 in 10 wells and distribution of the Tamrau, Woniwogi, Jass, demu and Lelinta
1004 Formations, and Piniya Mudstone.

1005

1006 Figure 15. Palaeogeographic reconstruction of western New Guinea during the Late
1007 Cretaceous. Based on evidence from Late Cretaceous aged sediments encountered
1008 in 40 wells, 6 outcrop samples and distribution of the Tamrau and Jass formations,
1009 Amiri and Ekmai Sandstones, Piniya Mudstone, Imskin Limestone and Korido
1010 Metamorphics.

1011

1012 Figure 16. Age-diagnostic Late Cretaceous planktonic foraminifera, and key
1013 palaeoenvironmental indicators, observed in outcrop samples. A-D) Carinate
1014 morphologies indicative of water depths greater than 100m. E-F) Globular planktonic
1015 foraminifera. Key - *Globotruncana* spp.(G), *Globotruncanita conica* (G.c),
1016 *Globotruncana arca* (G.a), *Abathomphalus mayaroensis* (A.m), *Heterohelix* spp. (H).

1017

1018 Figure 17. Palaeogeographic reconstruction of western New Guinea during the
1019 Paleocene. Based on evidence from Paleocene aged sediments encountered in 30

1020 wells, 5 outcrop samples and distribution of the Waripi and Daram Formations, and
1021 Imskin Limestone.

1022

1023 Figure 18. Palaeogeographic reconstruction of western New Guinea during the Early
1024 Eocene. Based on evidence from Early Eocene aged sediments encountered in 25
1025 wells, 9 outcrop samples and distribution of the Faumai, Imskin and Lengguru
1026 Limestones.

1027

1028 Figure 19. Age-diagnostic Early Eocene foraminifera, and key palaeoenvironmental
1029 indicators, observed in outcrop samples. A-E) Large, flat, rotaliine foraminifera
1030 indicative of water depths between 20m and 50m from the Faumai Limestone. F)
1031 Globular planktonic foraminifera indicative of water depths between 50m and 100m,
1032 Imskin limestone. G-H) Deep-water facies containing carinate planktonic foraminifera
1033 indicative of water depths in excess of 100m, Imskin Limestone. Key - *Alveolina* spp.
1034 (*A*), *Asterocyclina* spp. (*As*), *Alveolina subpyrenaica* (*A.s*), *Discocyclina ranikotensis*
1035 (*D.r*), *Alveolina globosa* (*A.g*), *Operculina* spp. (*O*), *Cuvillierina* spp. (*C*), *Acarinina*
1036 spp. (*Ac*), *Globigerinatheka* spp. (*Gt*), *Morozovella* spp. (*Mz*).

1037

1038 Figure 20. Palaeogeographic reconstruction of western New Guinea during the
1039 Middle - Late Eocene. Based on evidence from Middle - Late Eocene aged
1040 sediments encountered in 39 wells, 13 outcrop samples and distribution of the
1041 Faumai, Imskin and Lengguru Limestones, and Auwewa Formation.

1042

1043 Figure 21. Age-diagnostic Middle – Late Eocene foraminifera, and key
1044 palaeoenvironmental indicators, observed in outcrop samples. A-B) Shallow water

1045 facies from the Faumai Limestone. C-D) Shallow water facies observed in limestone
1046 lenses of the Auwewa Formation from Supiori. E-G) Globular planktonic foraminifera
1047 indicative of water depths between 50m and 100m, Imskin Limestone. H) Deep-
1048 water facies containing carinate planktonic foraminifera indicative of water depths
1049 greater than 100m, Imskin Limestone. Key – *Nummulites gizehensis* (N.g),
1050 *Pellatispirella* spp. (Pt), *Acarinina* spp. (Ac), *Globigerinatheka* spp. (Gt), *Subbotina*
1051 spp. (Sb), *Morozovella* spp. (Mz).

1052

1053 Figure 22. Palaeogeographic reconstruction of western New Guinea during the
1054 Oligocene. Based on evidence from Oligocene aged sediments encountered in 25
1055 wells, 6 outcrop samples and distribution of the Sirga Formation.

1056

1057 Figure 23. Palaeogeographic reconstruction of western New Guinea during the Early
1058 Miocene. Based on evidence from Early Miocene aged sediments encountered in 48
1059 wells, 37 outcrop samples and distribution of the Koor, Kais and Maruni Limestones,
1060 and Wainukendi, Wafordori and Wurui Formations.

1061

1062 Figure 24. Age-diagnostic Early Miocene foraminifera, and key palaeoenvironmental
1063 indicators, observed in outcrop samples. A-D) Shallow water, reefal, grainstones of
1064 the Maruni Limestone. E) Shallow water packstone of the Kais Limestone. F) Large,
1065 flat, rotalines indicate water depths between 20m and 50m in the Maruni Limestone.
1066 Key – *Lepidocyclina sumatrensis* (L.s), *Lepidocyclina brouweri* (L.b), *Lepidocyclina*
1067 *oneatensis* (L.o), *Miogypsina tani* (M.t), *Spiroclypeus tidoenganensis* (S.t),
1068 *Eulepidina* spp. (Eu), *Miogypsina* spp. (Mg), *Amphistegina* spp. (Am), *Heterostegina*
1069 spp. (Hs).

1070

1071 Figure 25. Palaeogeographic reconstruction of western New Guinea during the
1072 Middle Miocene. Based on evidence from Middle Miocene aged sediments
1073 encountered in 55 wells, 42 outcrop samples and distribution of the Koor, Kais and
1074 Maruni Limestones, and Wainukendi, Wafordori and Napisendi Formations, and
1075 Sumboi Marl.

1076

1077 Figure 26. Age-diagnostic Middle Miocene foraminifera, and key
1078 palaeoenvironmental indicators, observed in outcrop samples. A) Large, flat,
1079 rotaliines indicating water depths between 20m and 50m from the Maruni Limestone.
1080 B) Shallow water wackestone containing taxa indicative of water depths no greater
1081 than 20m. C-D) Globular planktonic foraminifera indicating water depths between
1082 50m and 100m from near the top of the Maruni Limestone. Key – *Katacycloclypeus*
1083 *annulatus* (*K.a*), *Borelis melo* (*B.m*), *Globigerinoides* spp. (*Gd*), *Orbulina universa*
1084 (*O.u*).

1085

1086 Figure 27. Palaeogeographic reconstruction of western New Guinea during the Late
1087 Miocene. Based on evidence from Late Miocene aged sediments encountered in 65
1088 wells, 24 outcrop samples and distribution of the Klasafet and Befoor Formations.

1089

1090 Figure 28. Palaeogeographic reconstruction of western New Guinea during the Early
1091 Pliocene. Based on evidence from Early Pliocene aged sediments encountered in 66
1092 wells, 29 outcrop samples and distribution of the Klasman, Opmorai, Befoor, Wardo,
1093 Korem and Kurudu Formations, and the Wai Limestone.

1094

1095 Figure 29. Palaeogeographic reconstruction of western New Guinea during the Late
1096 Pliocene. Based on evidence from Late Pliocene aged sediments encountered in 62
1097 wells, 29 outcrop samples and distribution of the Opmorai Formation.

1098

1099 Figure 30. Palaeogeographic reconstruction of western New Guinea during the
1100 Pleistocene. Based on evidence from Pleistocene aged sediments encountered in 44
1101 wells, 5 outcrop samples and distribution of the Sele, Opmorai, Manokwari and
1102 Mokmer Formations, and Ansus Conglomerate.

1103

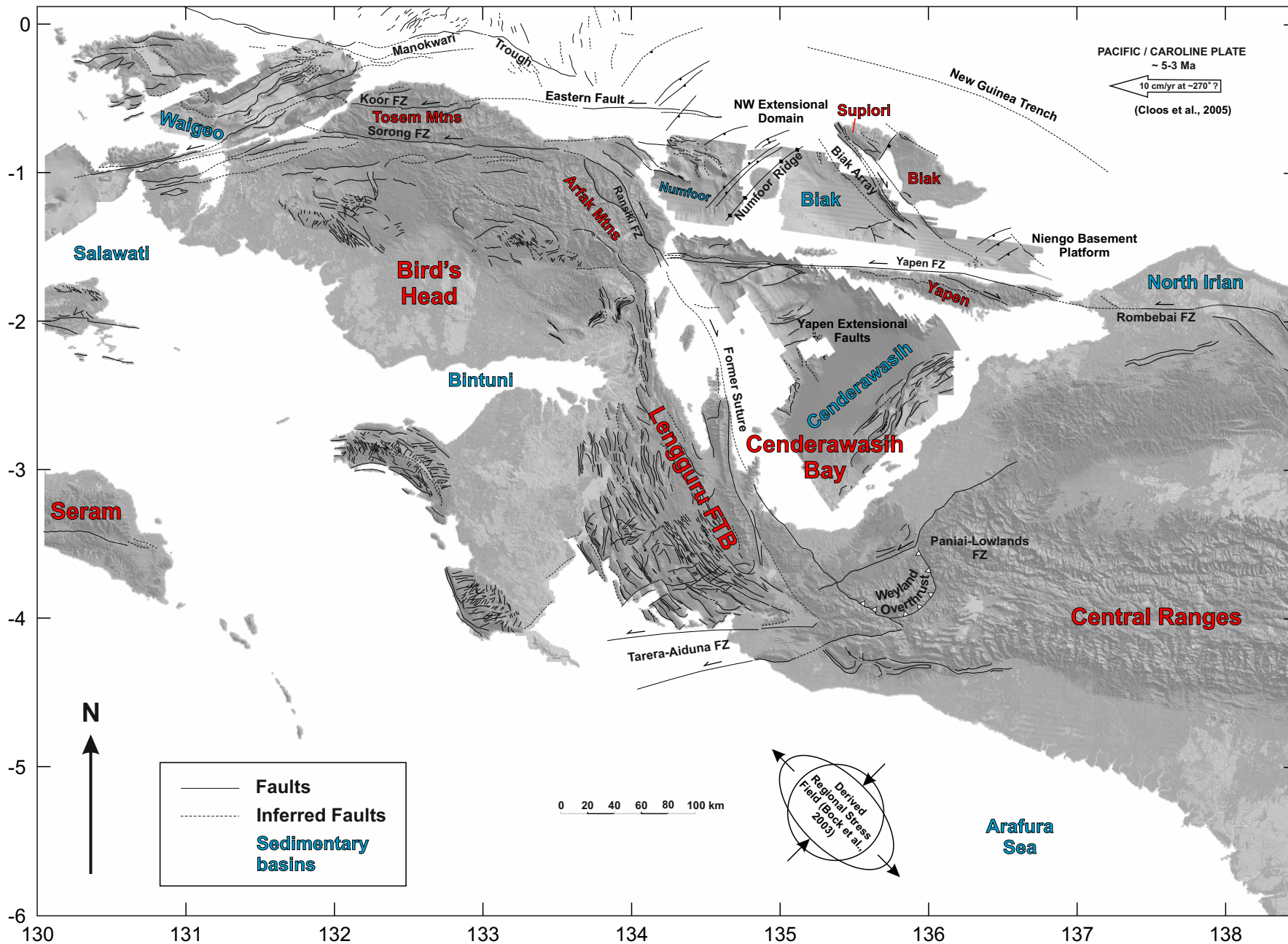


Figure 1

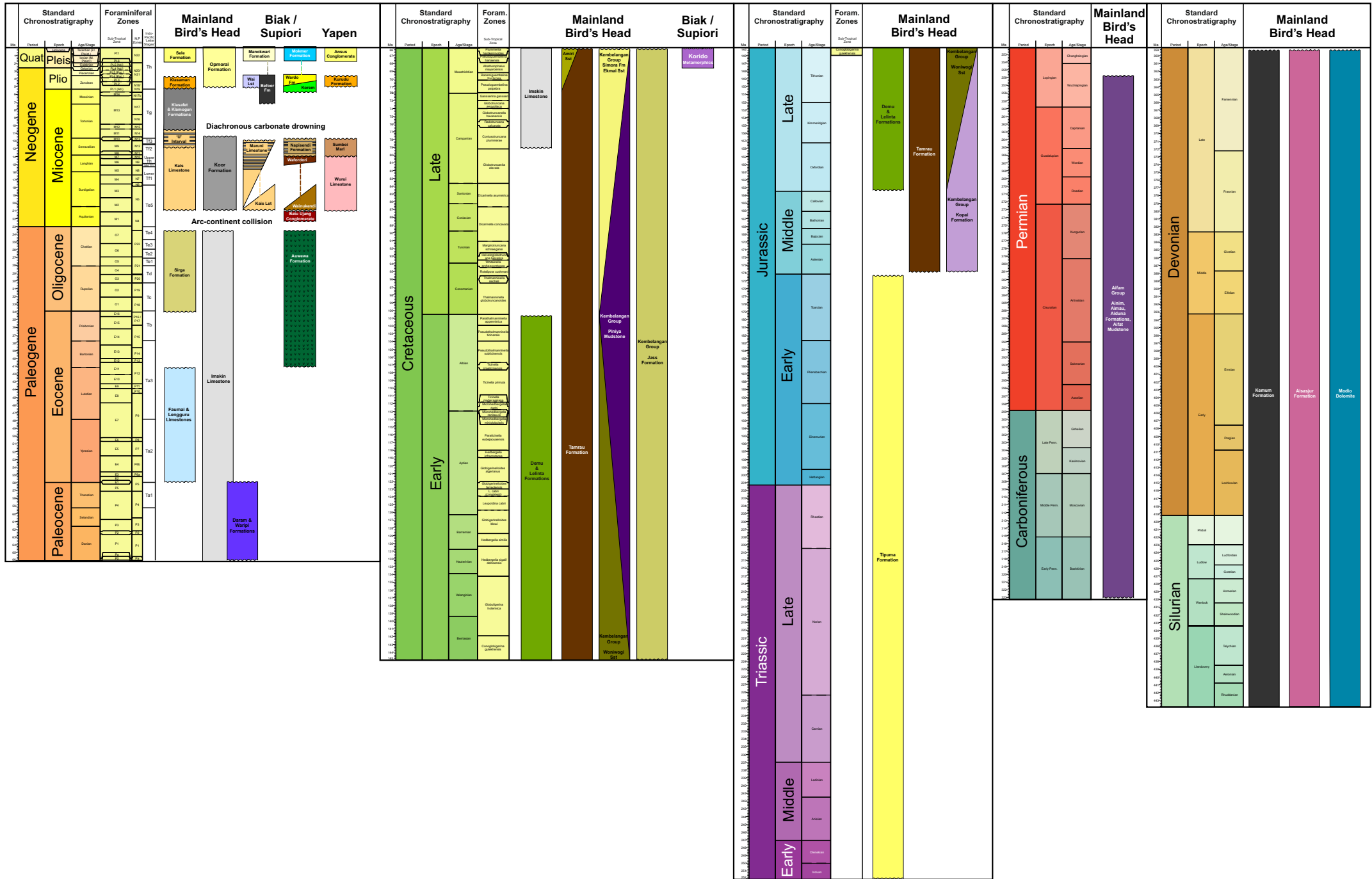


Figure 2

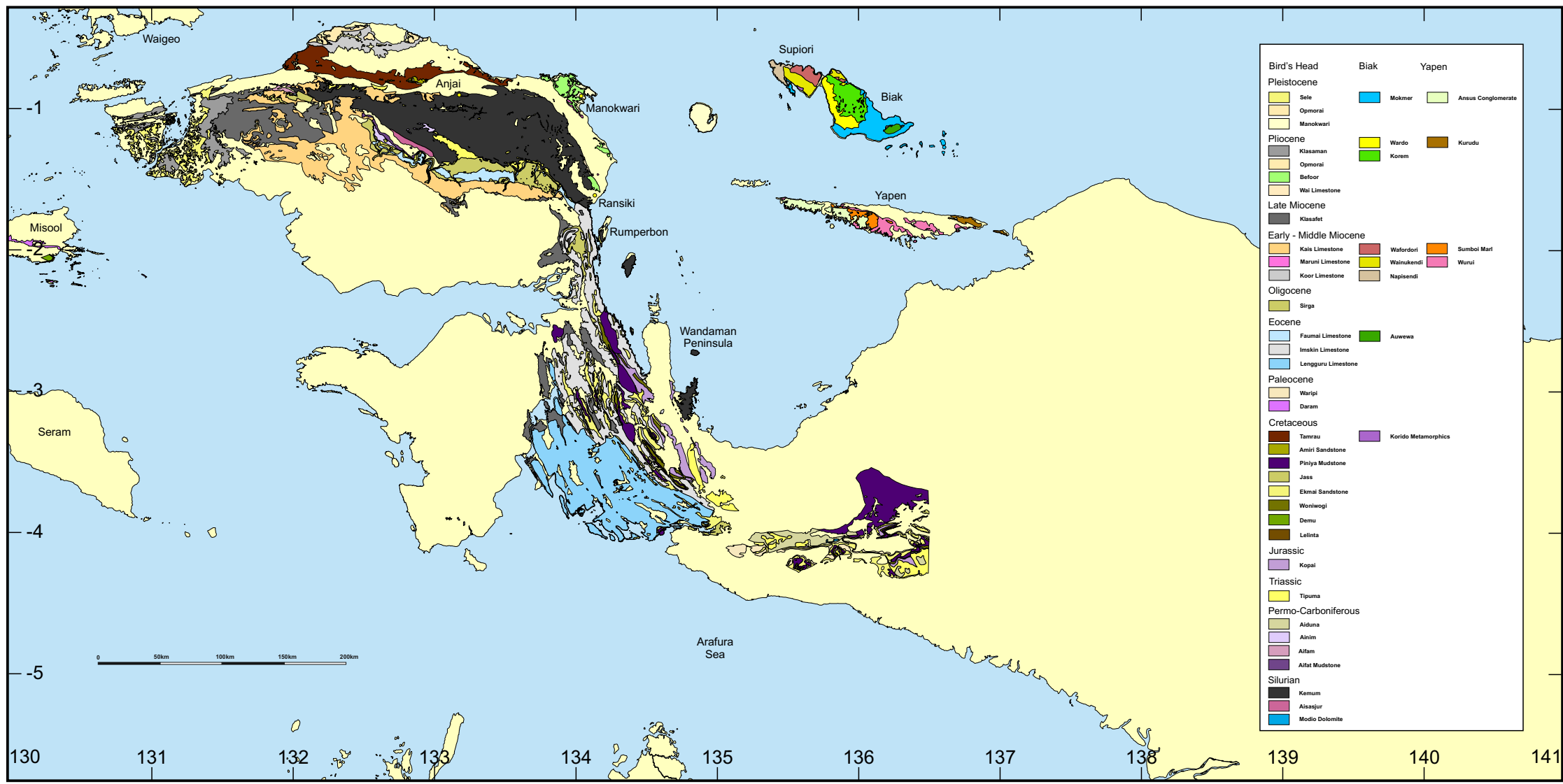


Figure 3

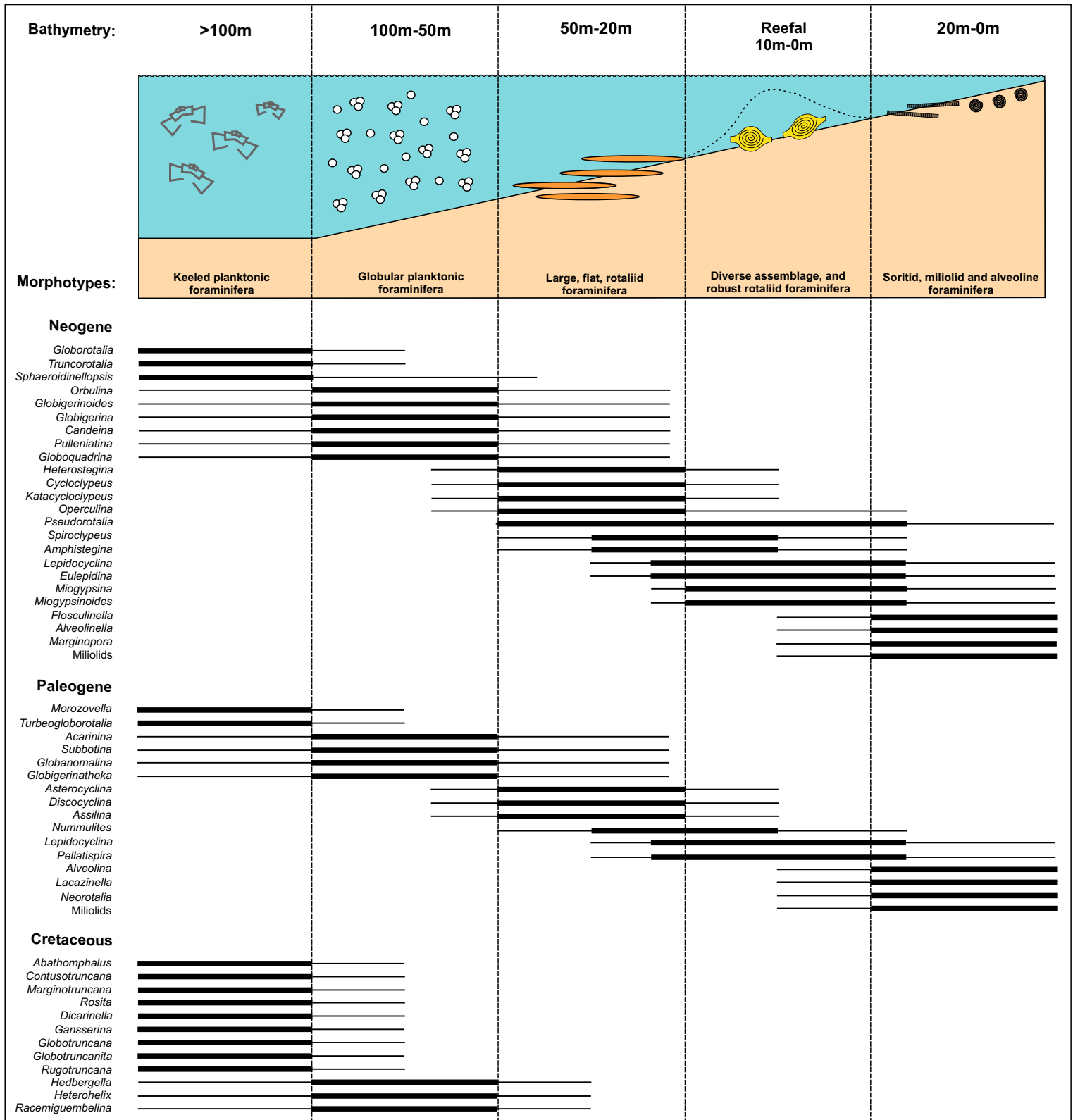
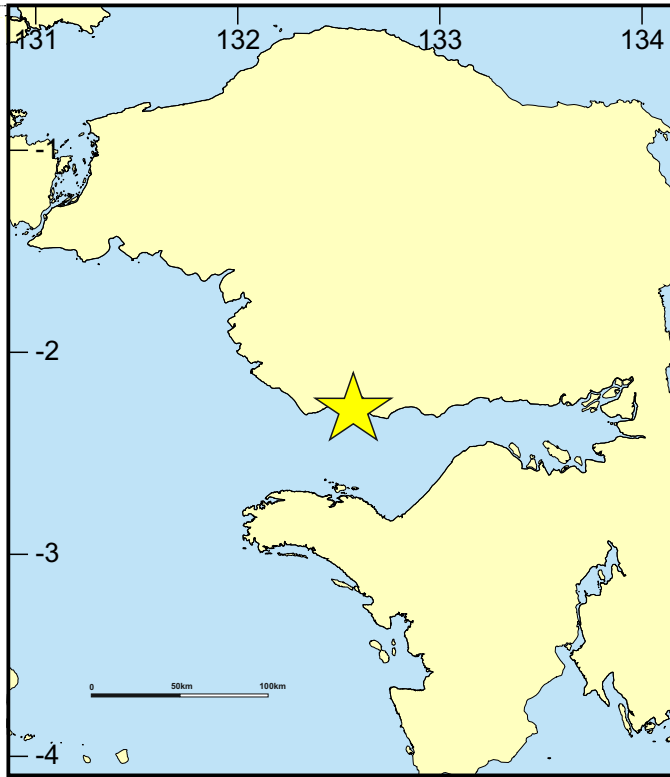


Figure 4



Recent
 Pleistocene
 Late Pliocene
 Early Pliocene
 Late Miocene
 Middle Miocene
 Early Miocene
 Oligocene
 M.-L. Eocene
 Early Eocene
 Paleocene
 Late Cretaceous
 Early Cretaceous
 Late Jurassic
 Middle Jurassic
 Early Jurassic
 Triassic
 Permian
 Carboniferous
 Silurian

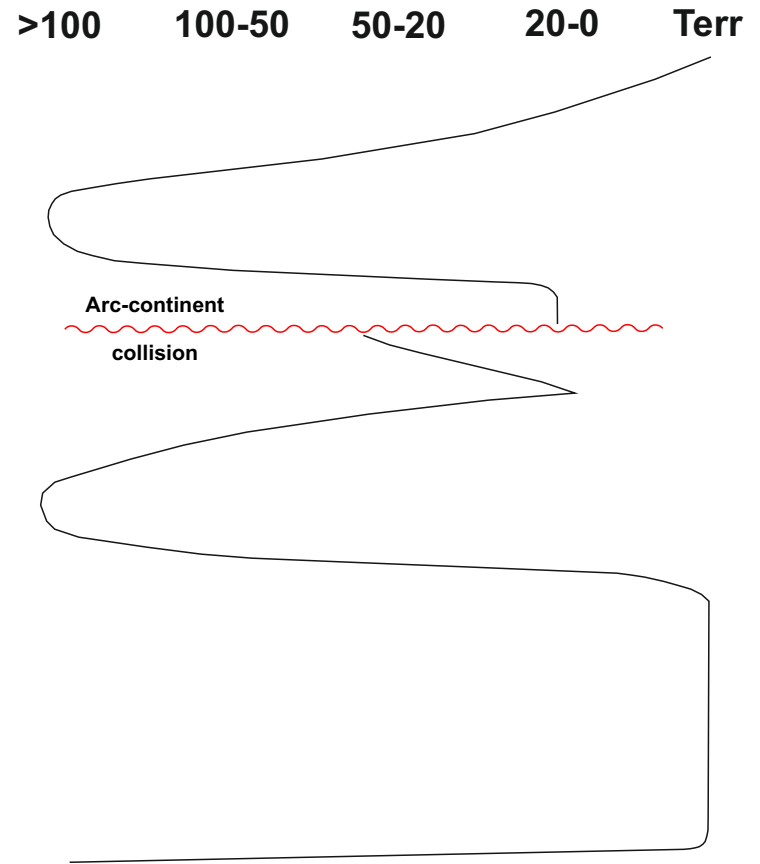


Figure 5

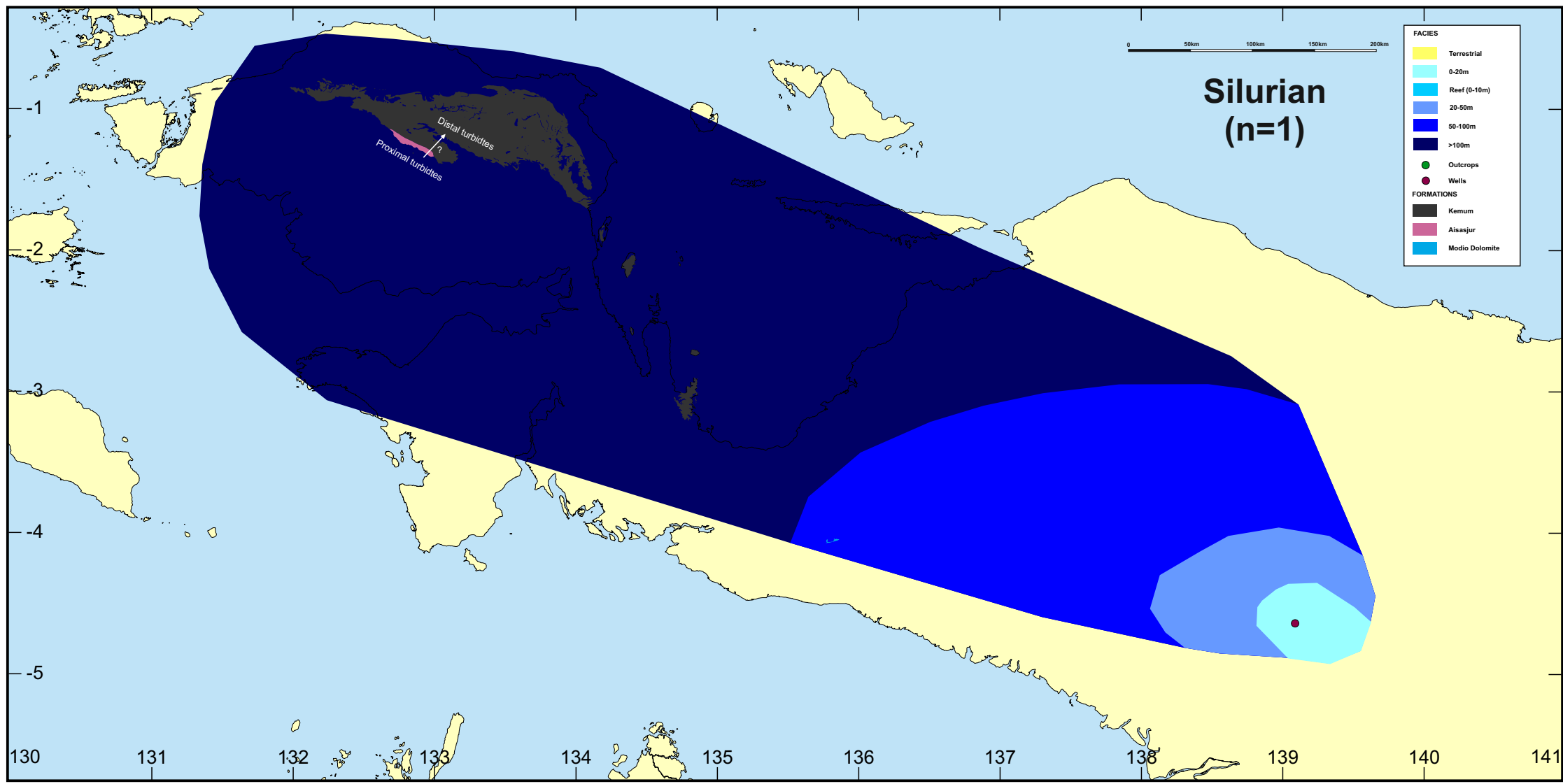


Figure 6

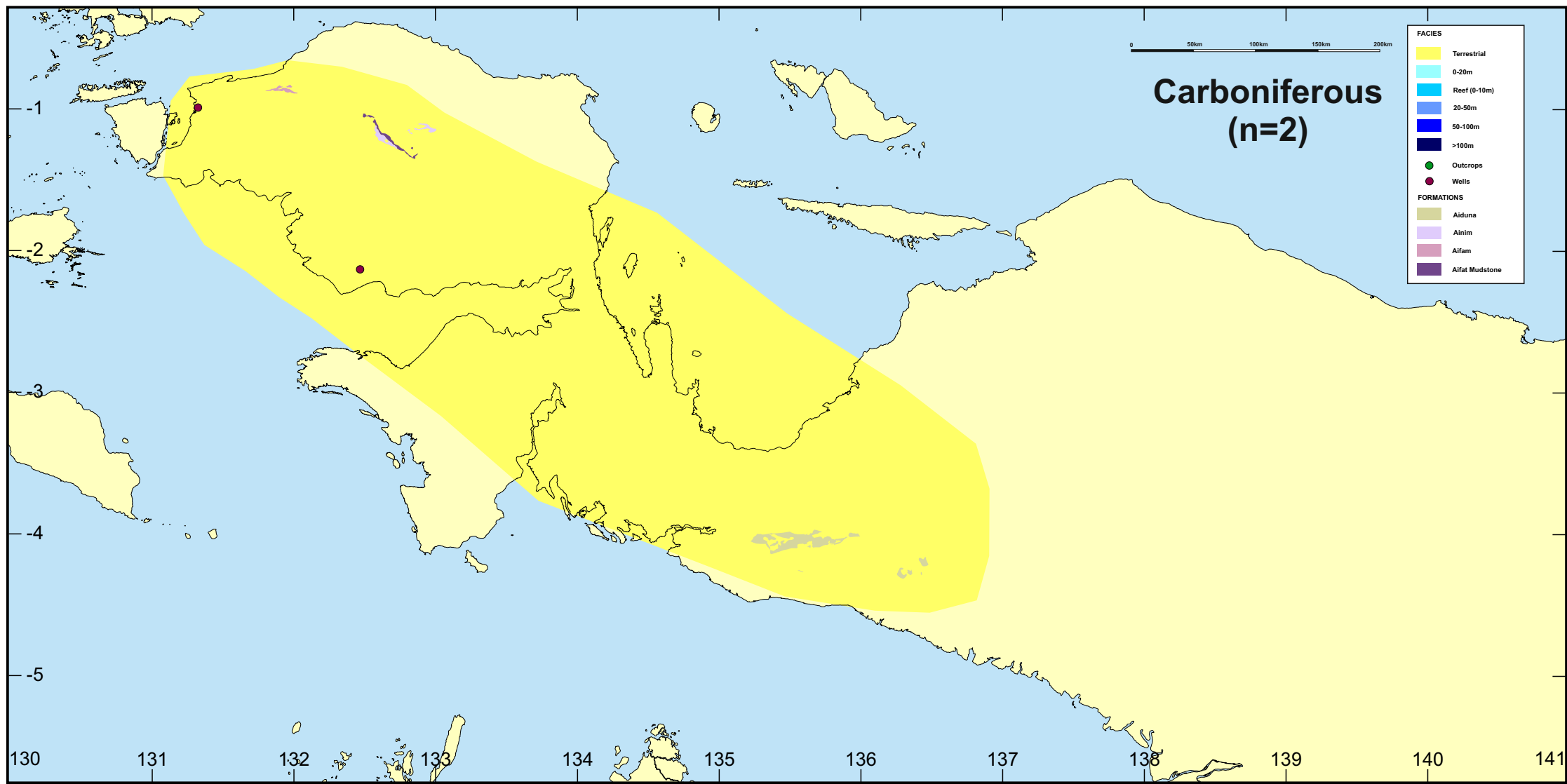


Figure 7

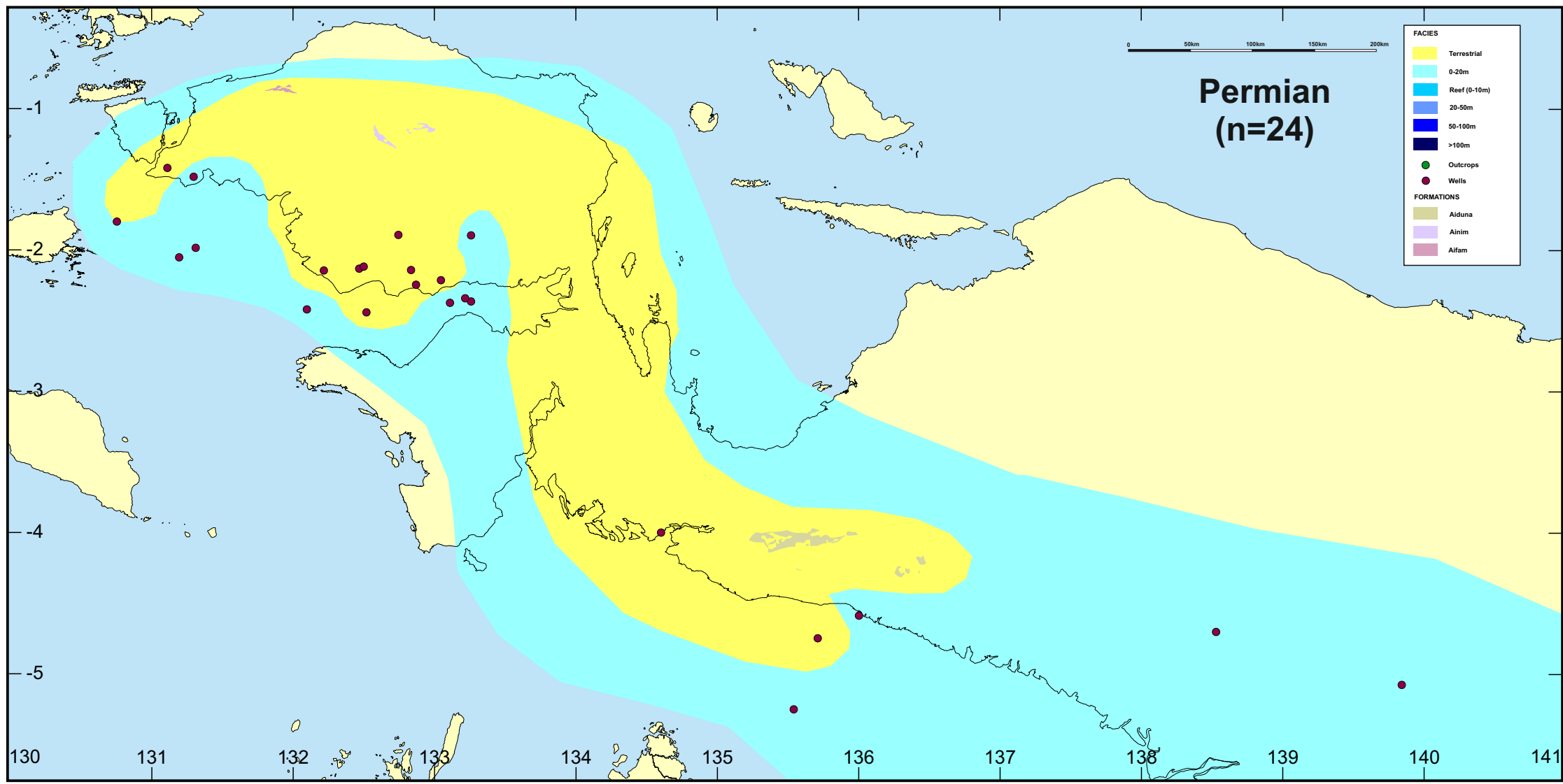


Figure 8

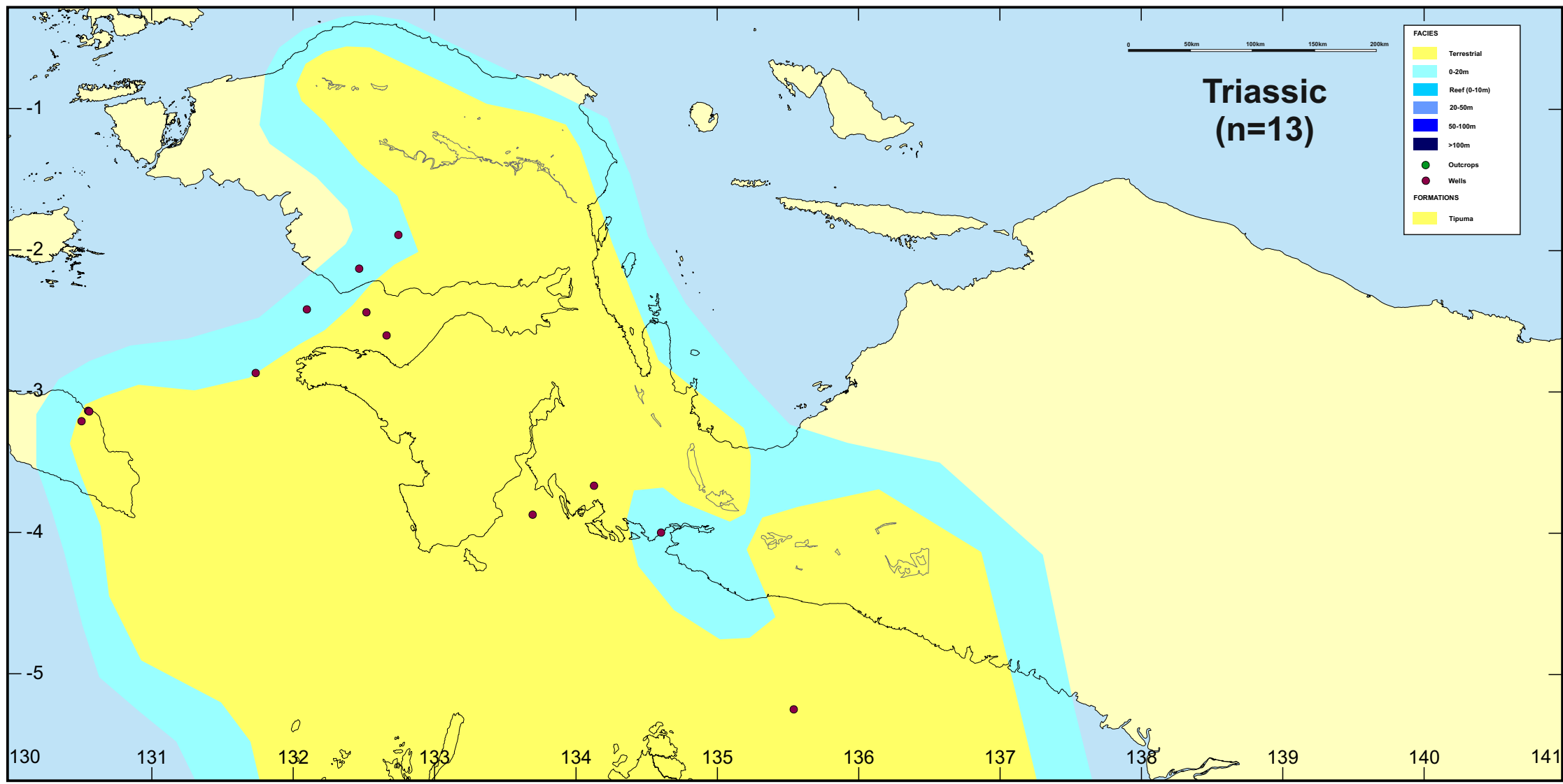


Figure 9

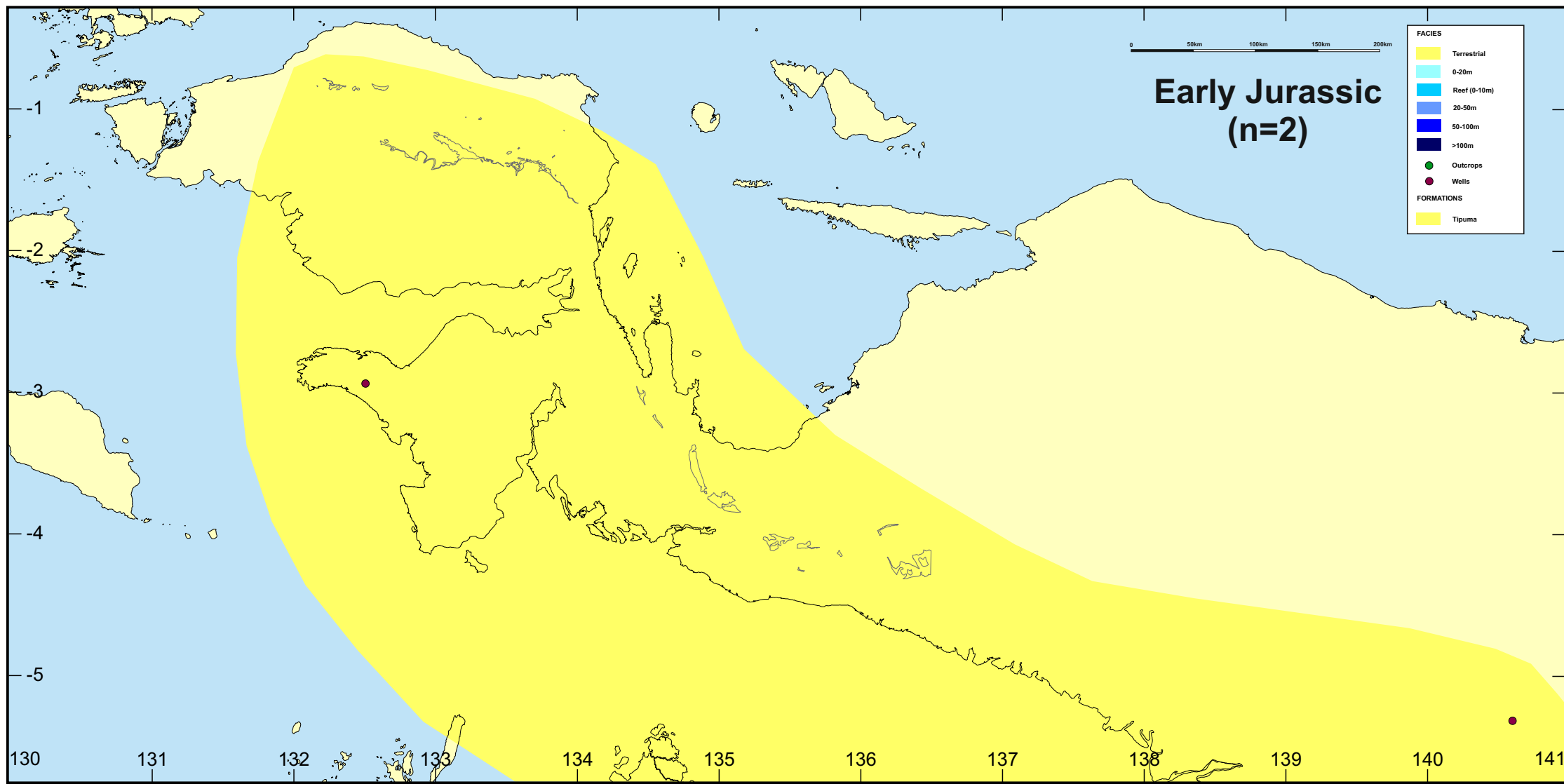


Figure 10

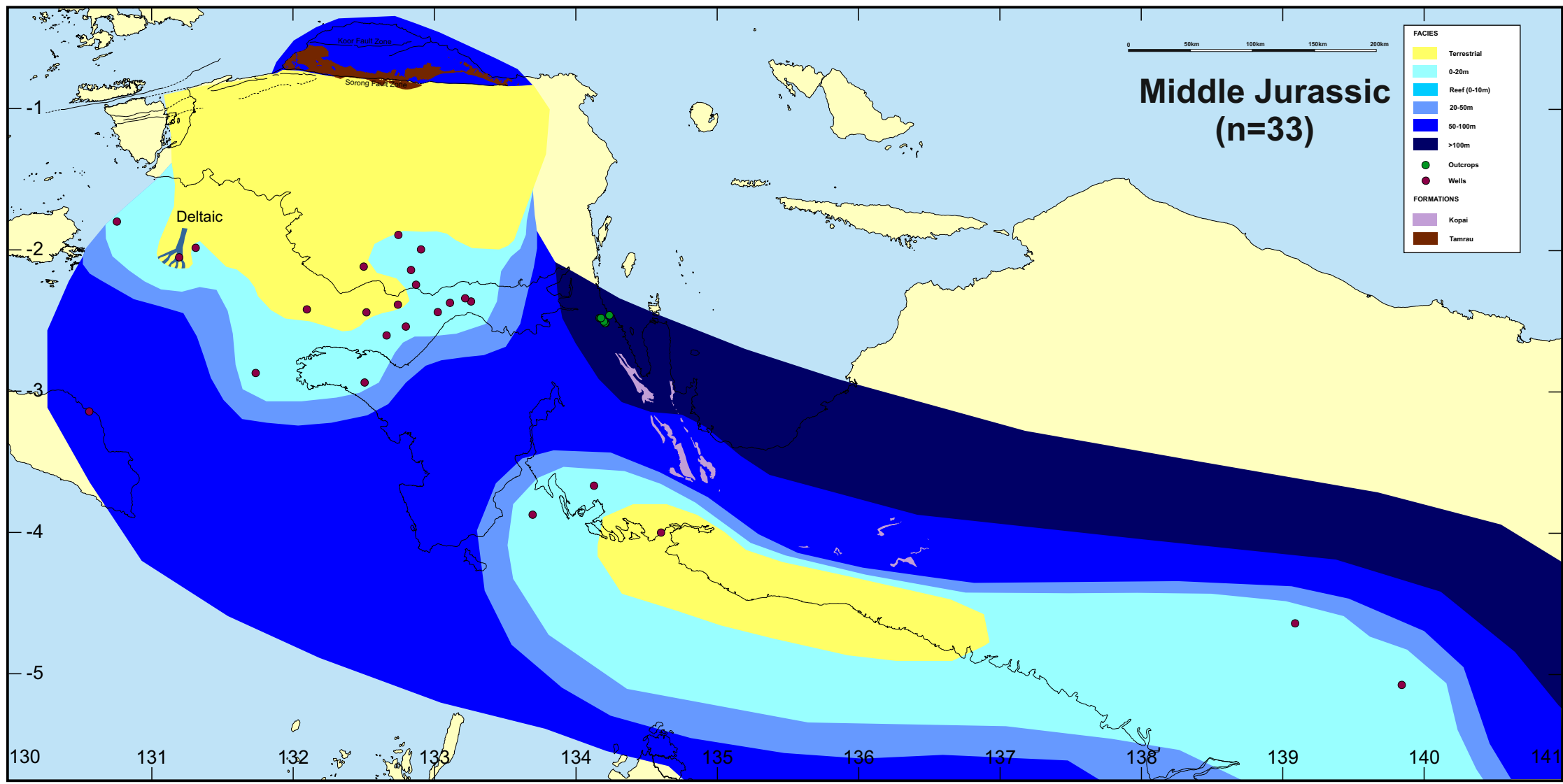


Figure 11



Figure 12

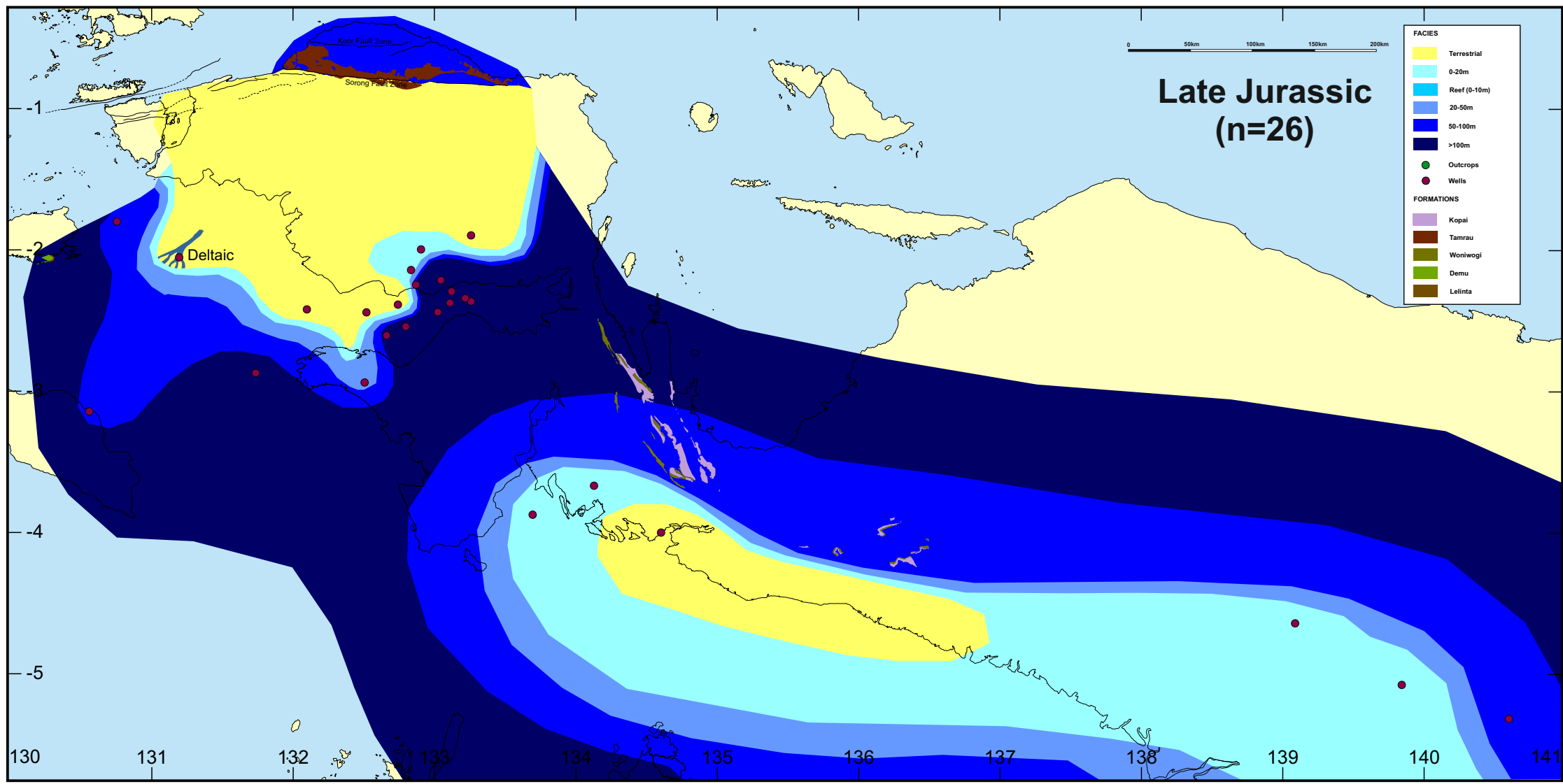


Figure 13

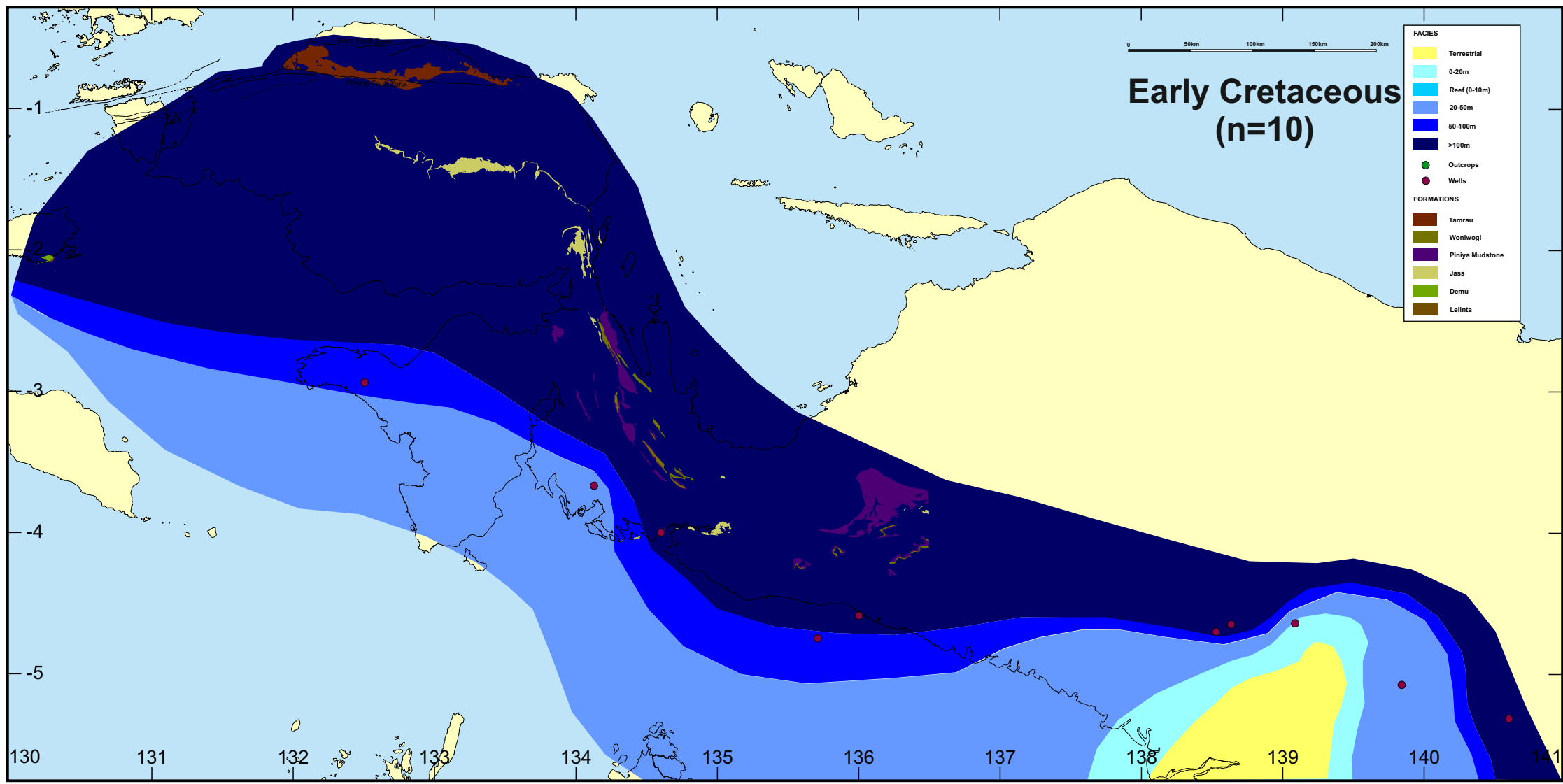


Figure 14

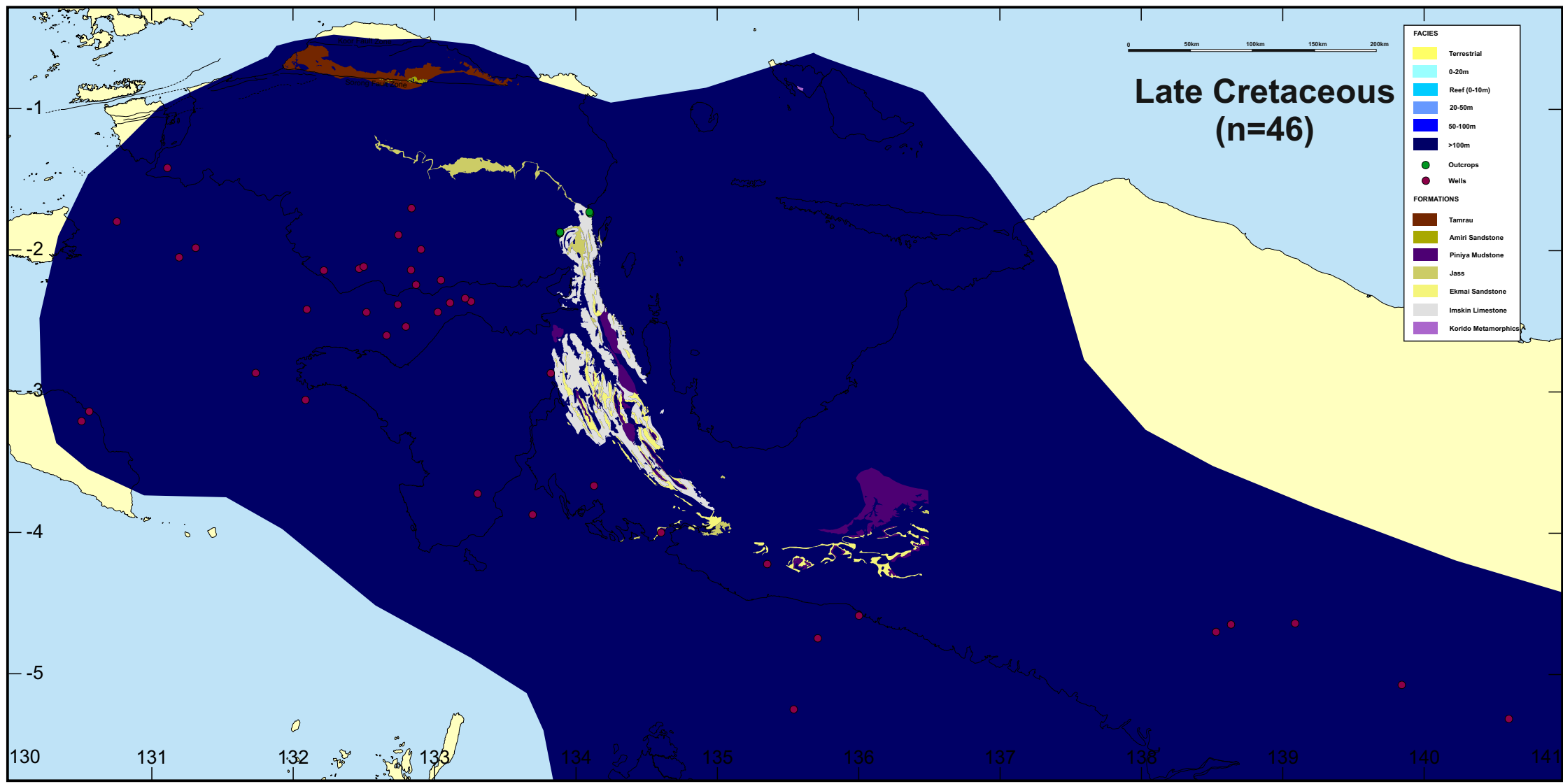


Figure 15

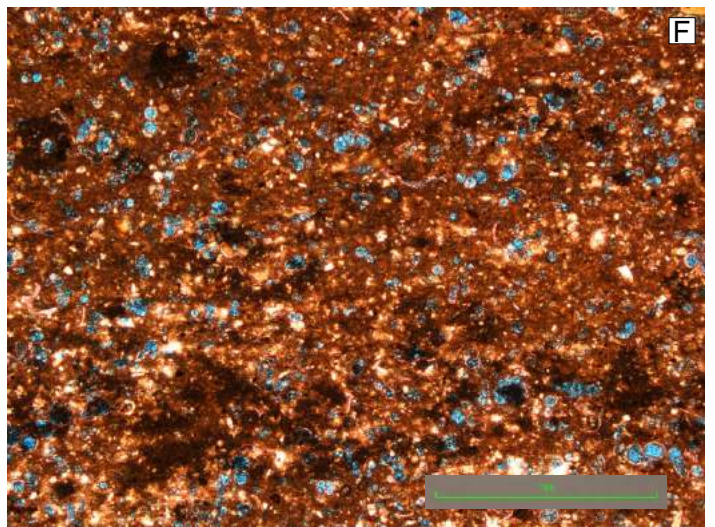
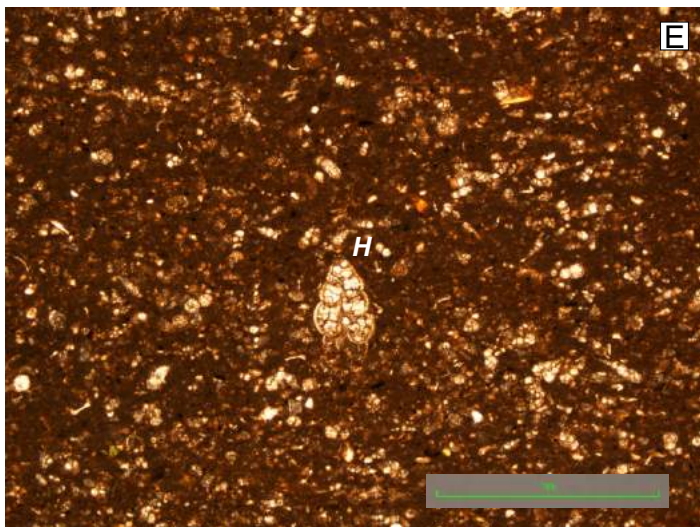
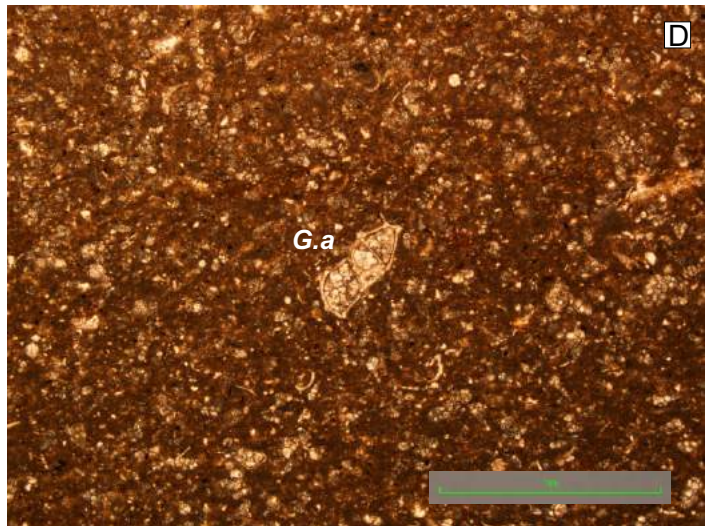
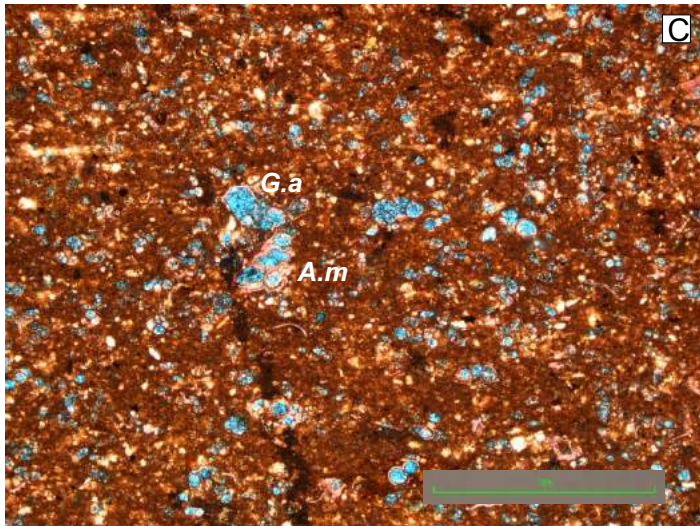
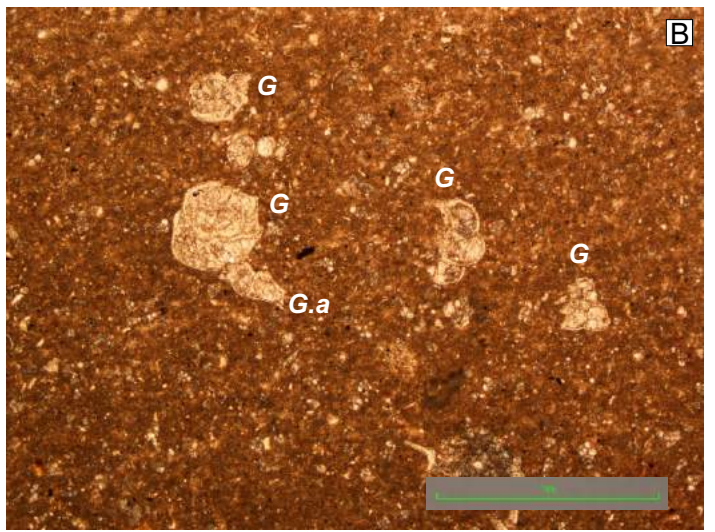
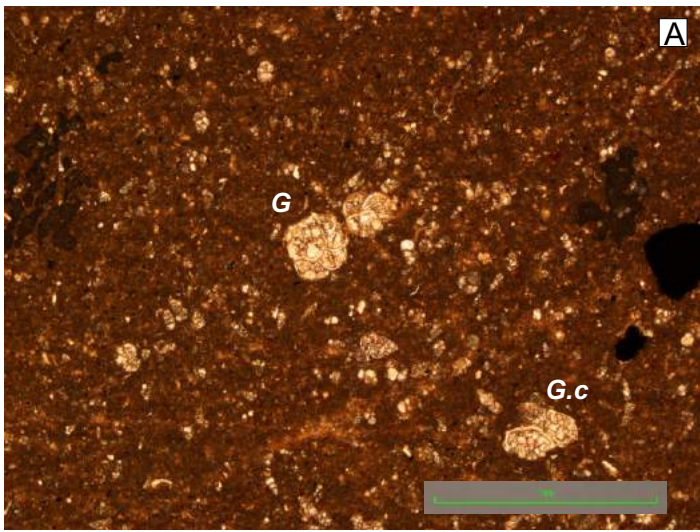


Figure 16

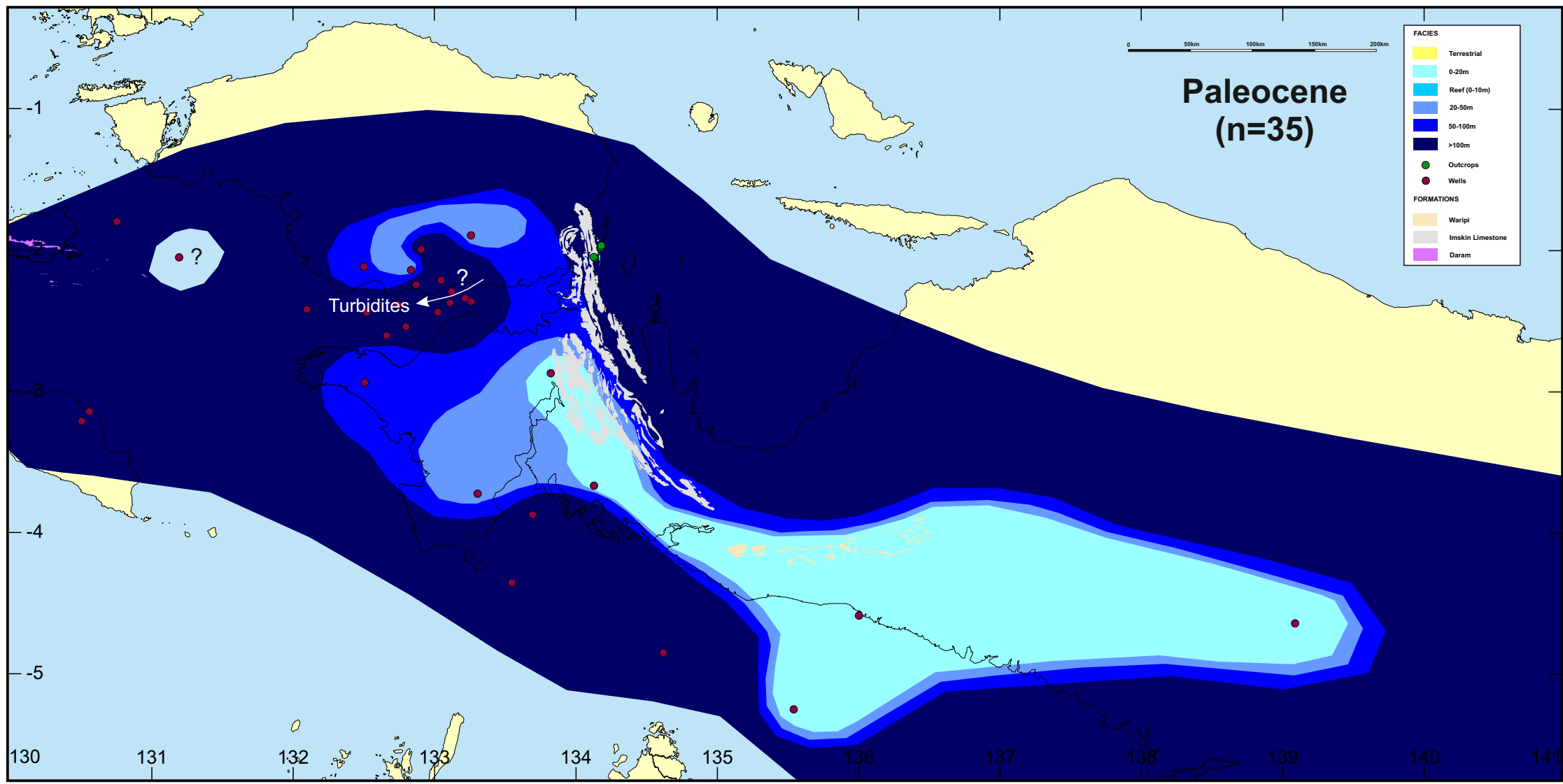


Figure 17

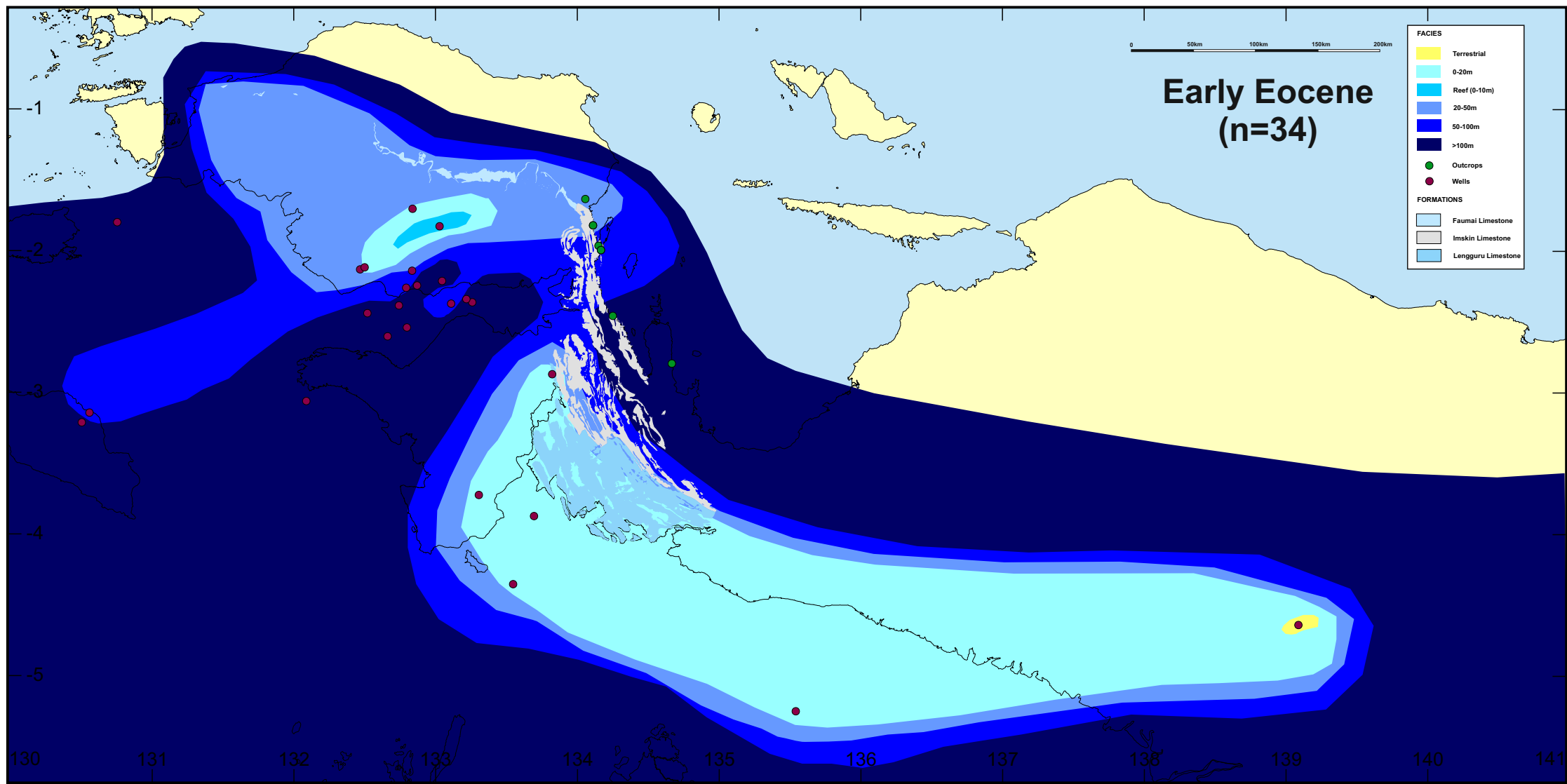


Figure 18

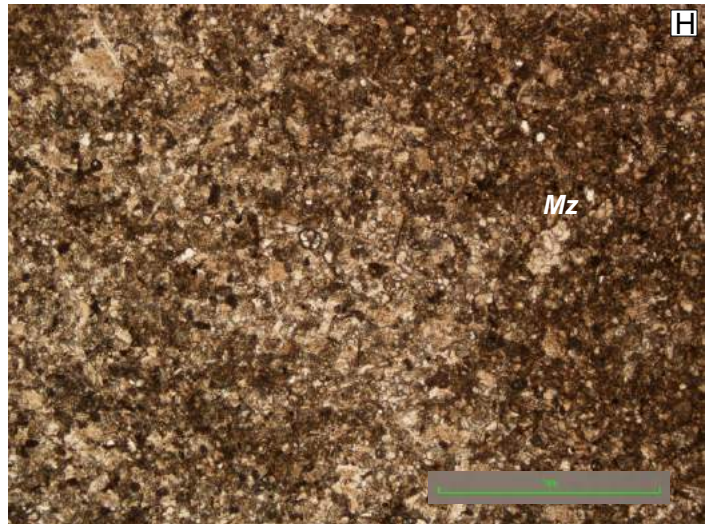
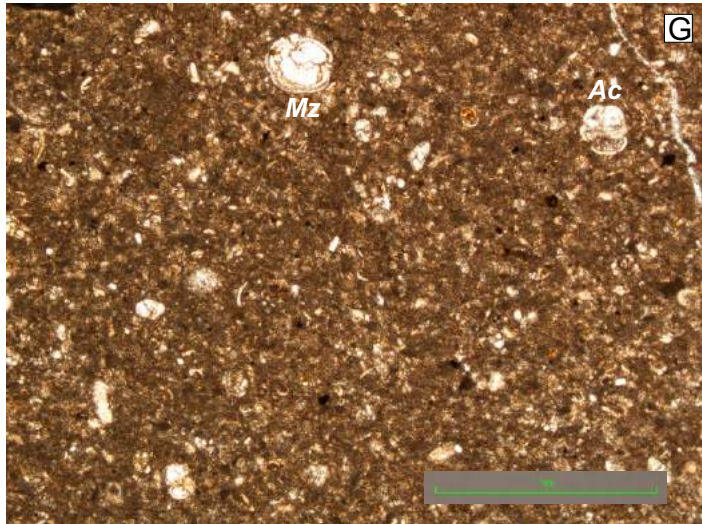
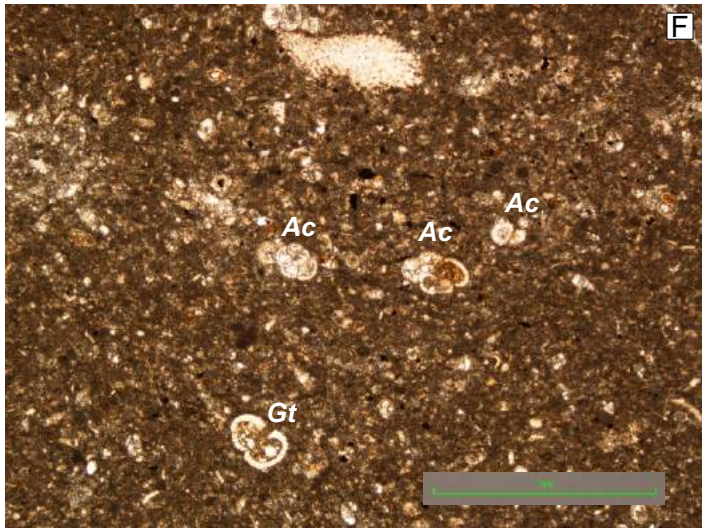
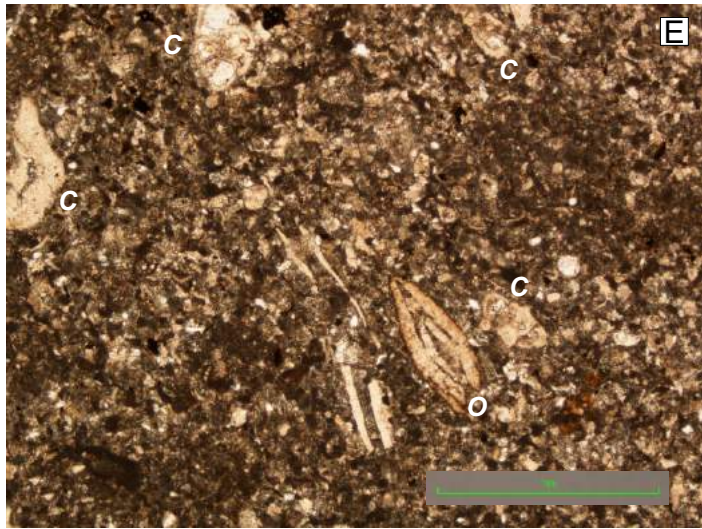
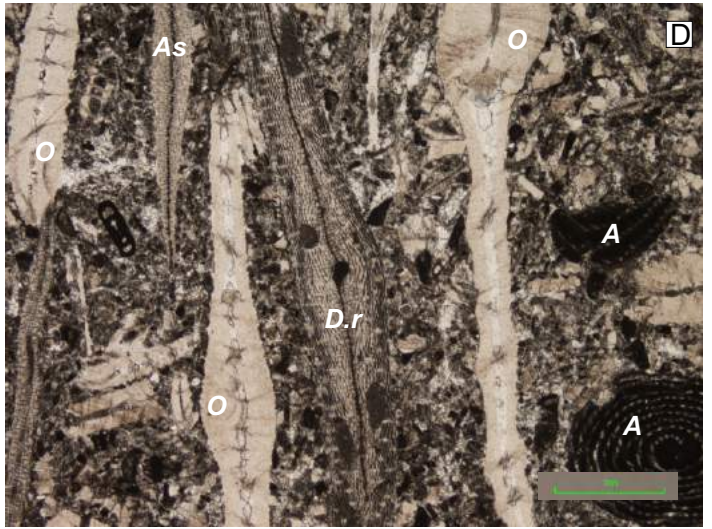
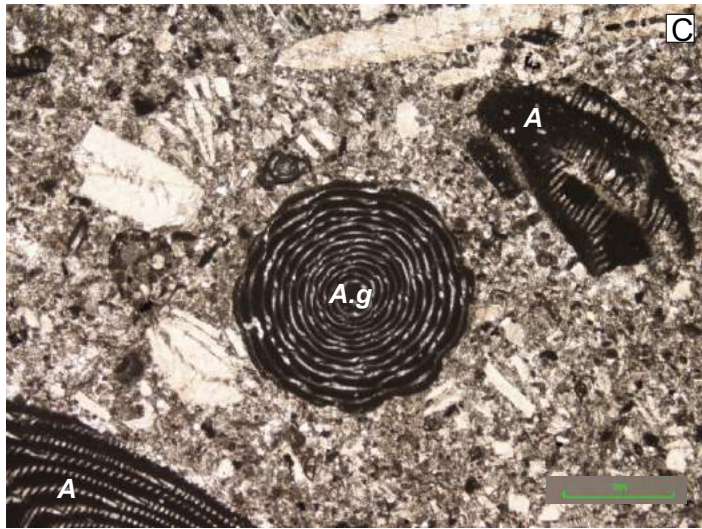
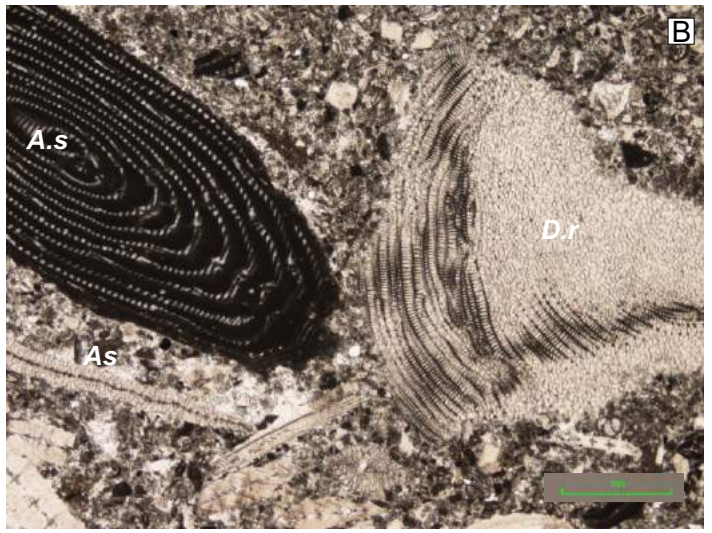
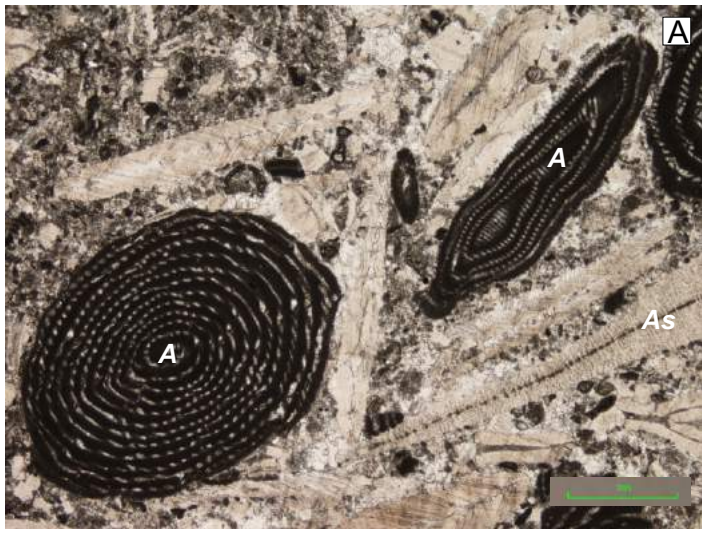


Figure 19

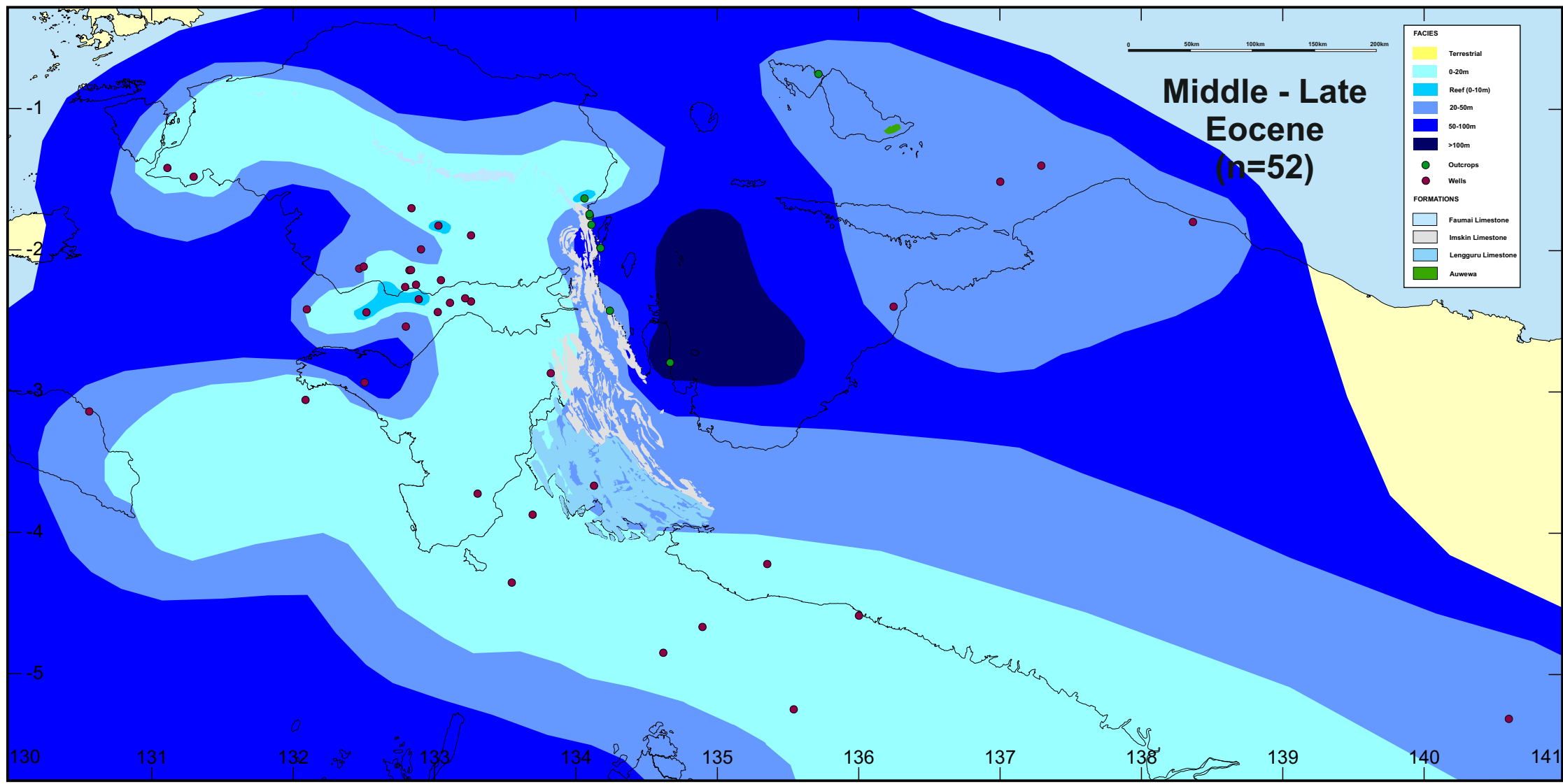


Figure 20

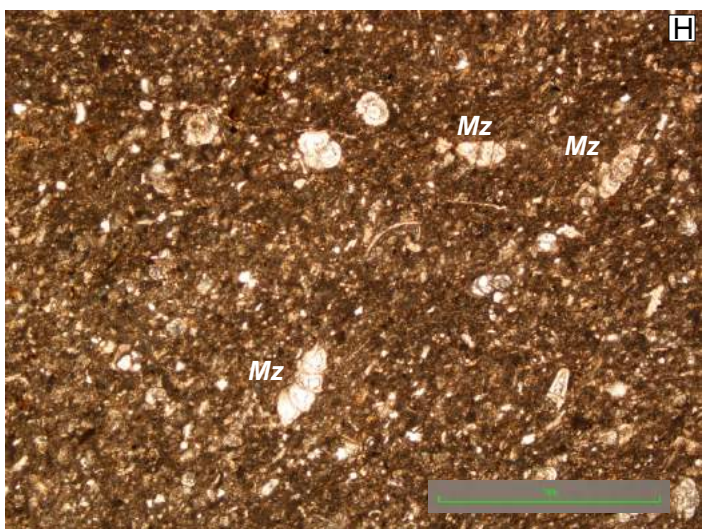
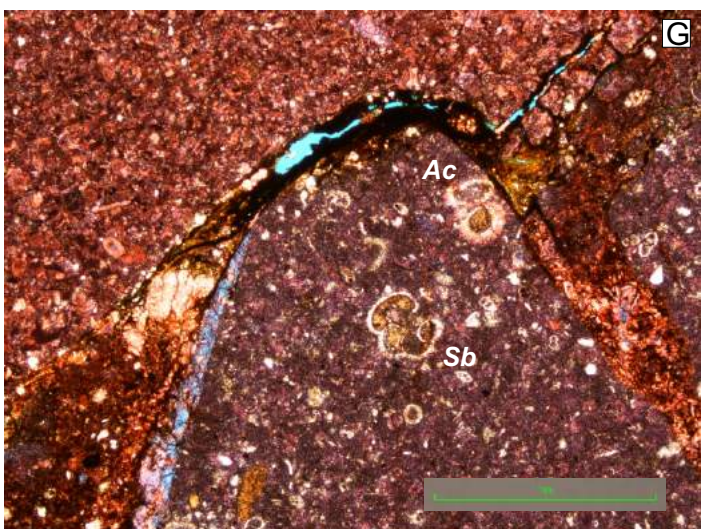
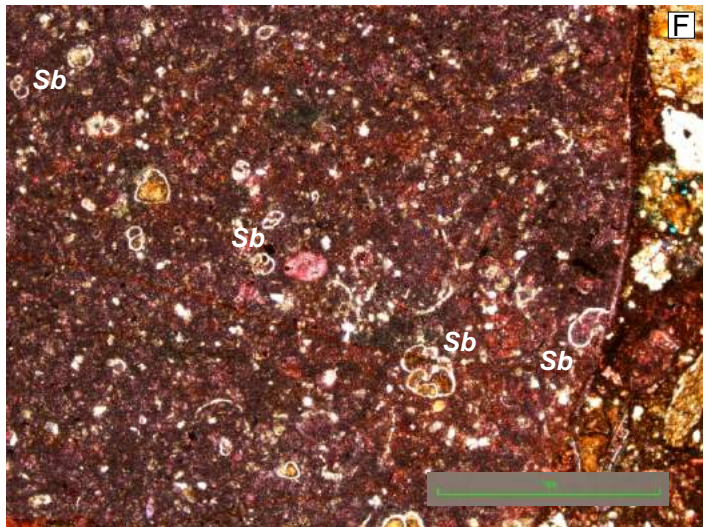
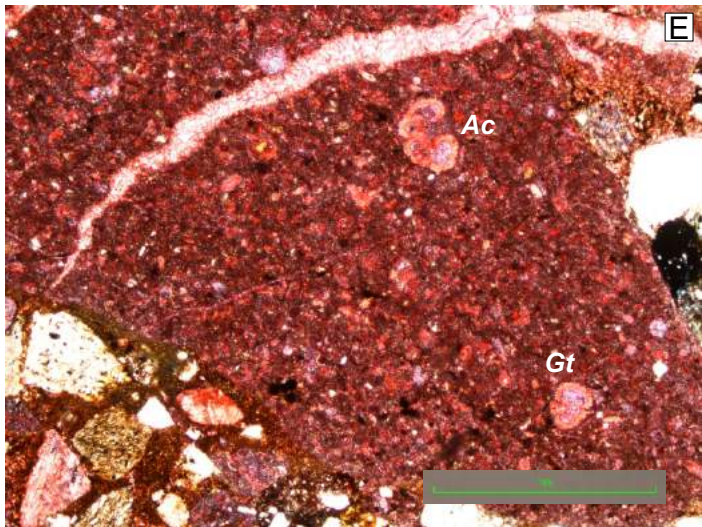
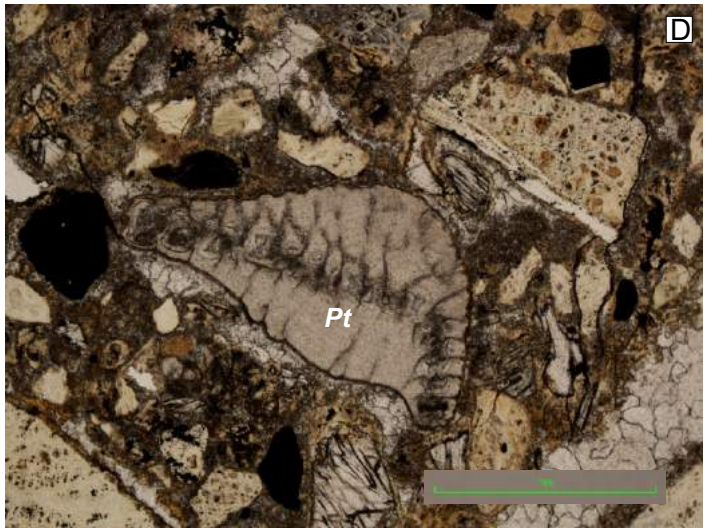
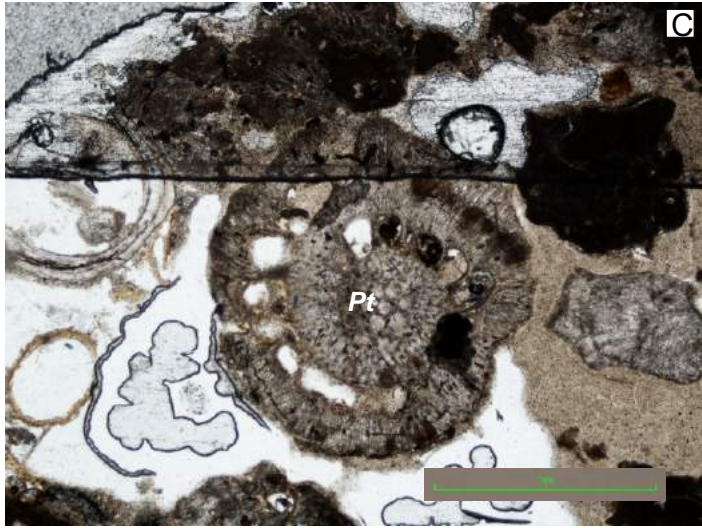
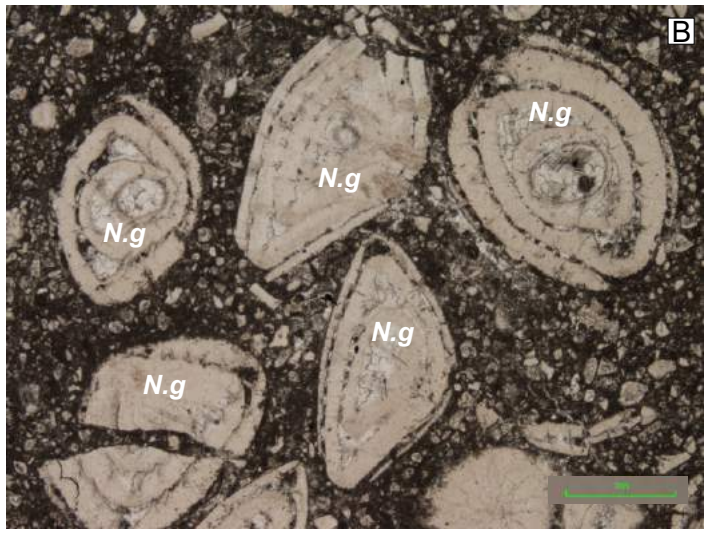
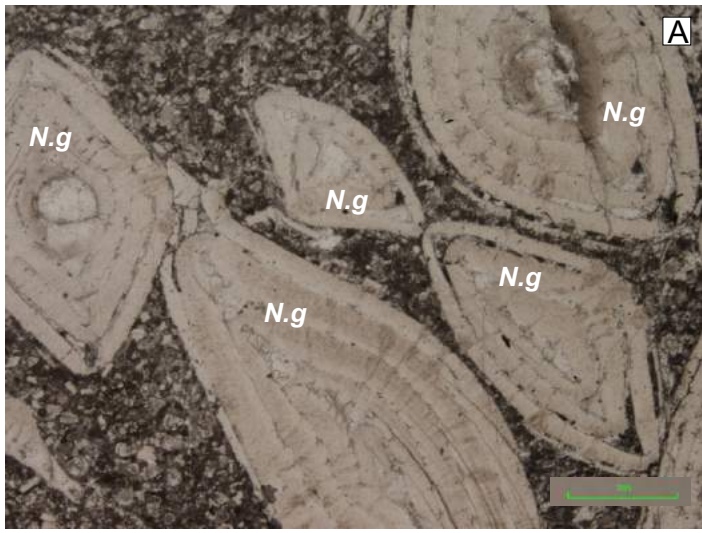


Figure 21

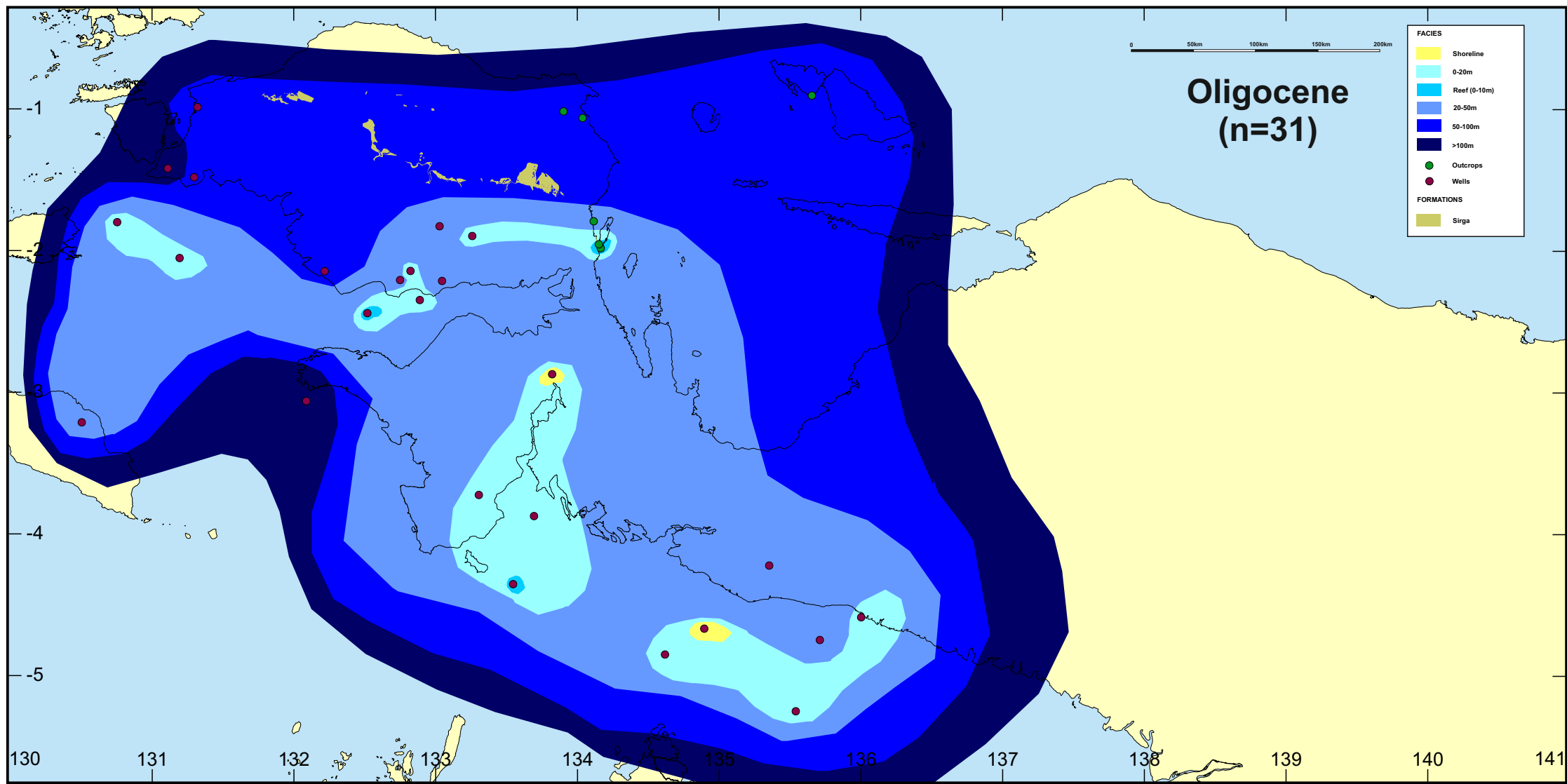


Figure 22

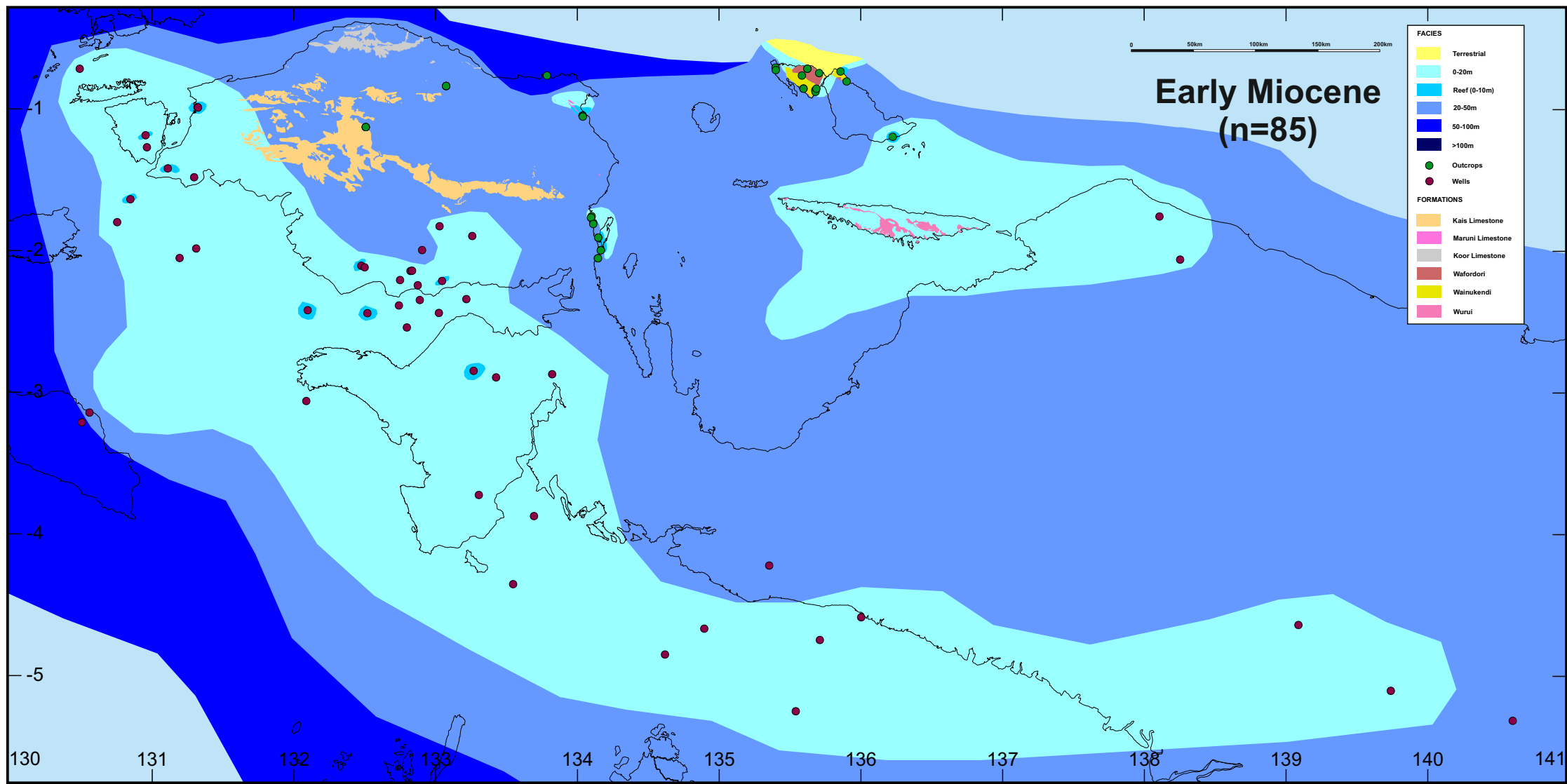


Figure 23

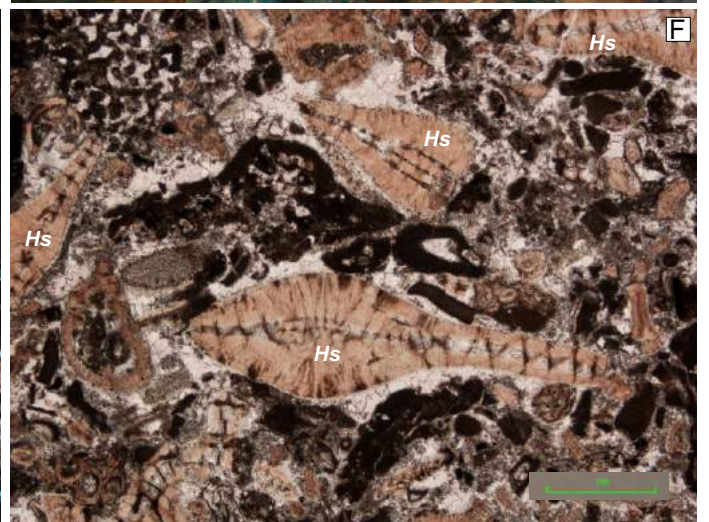
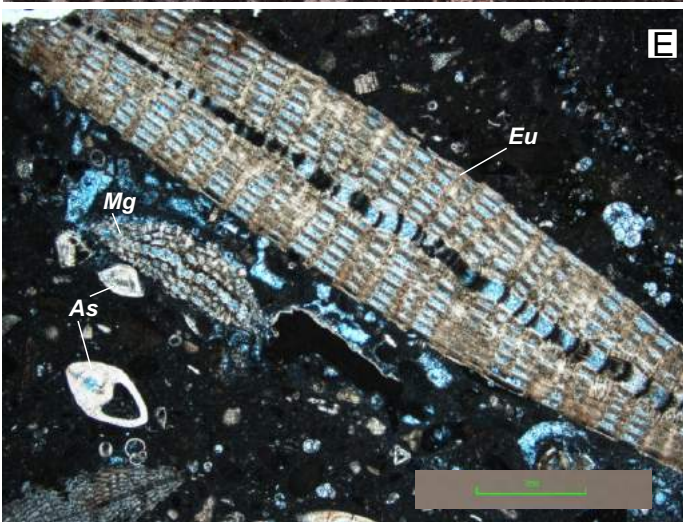
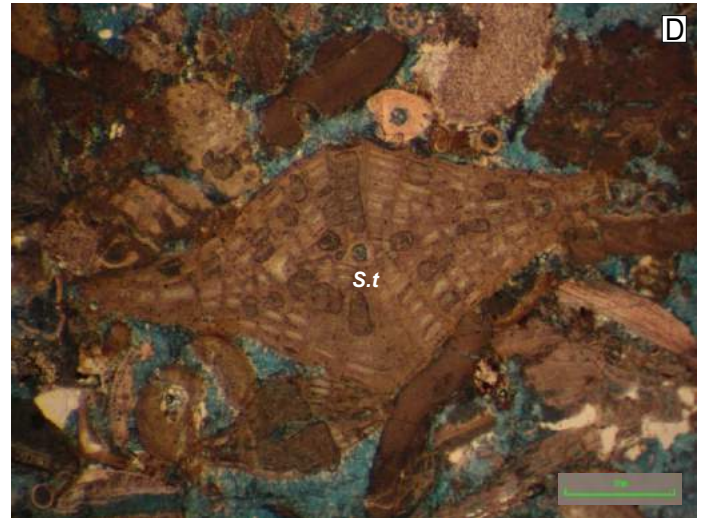
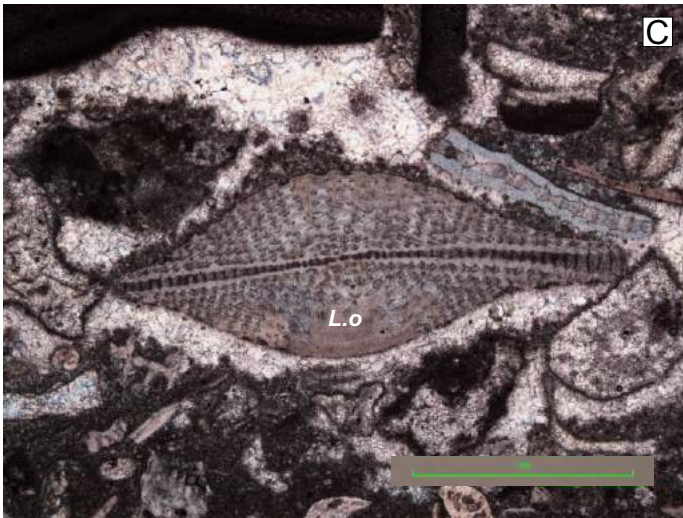
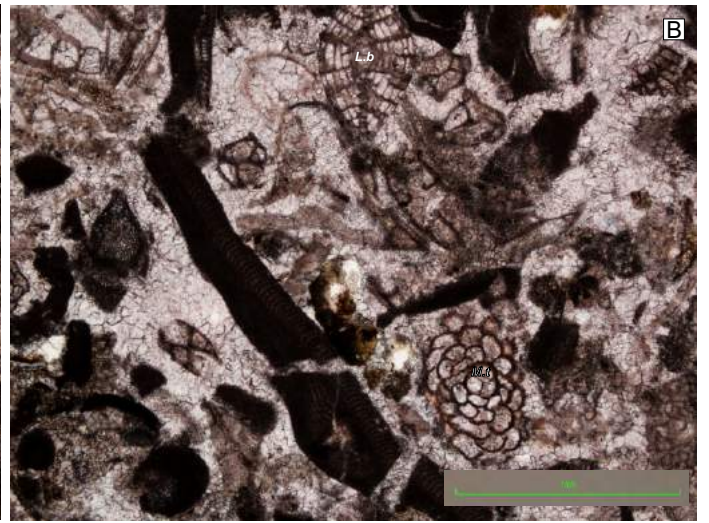
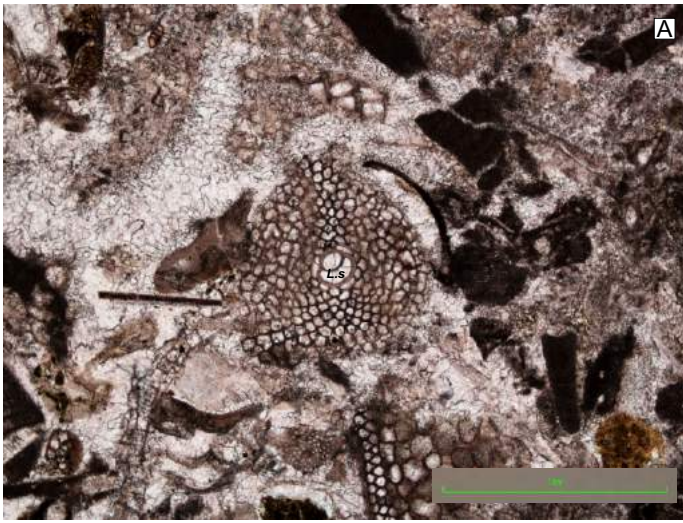


Figure 24

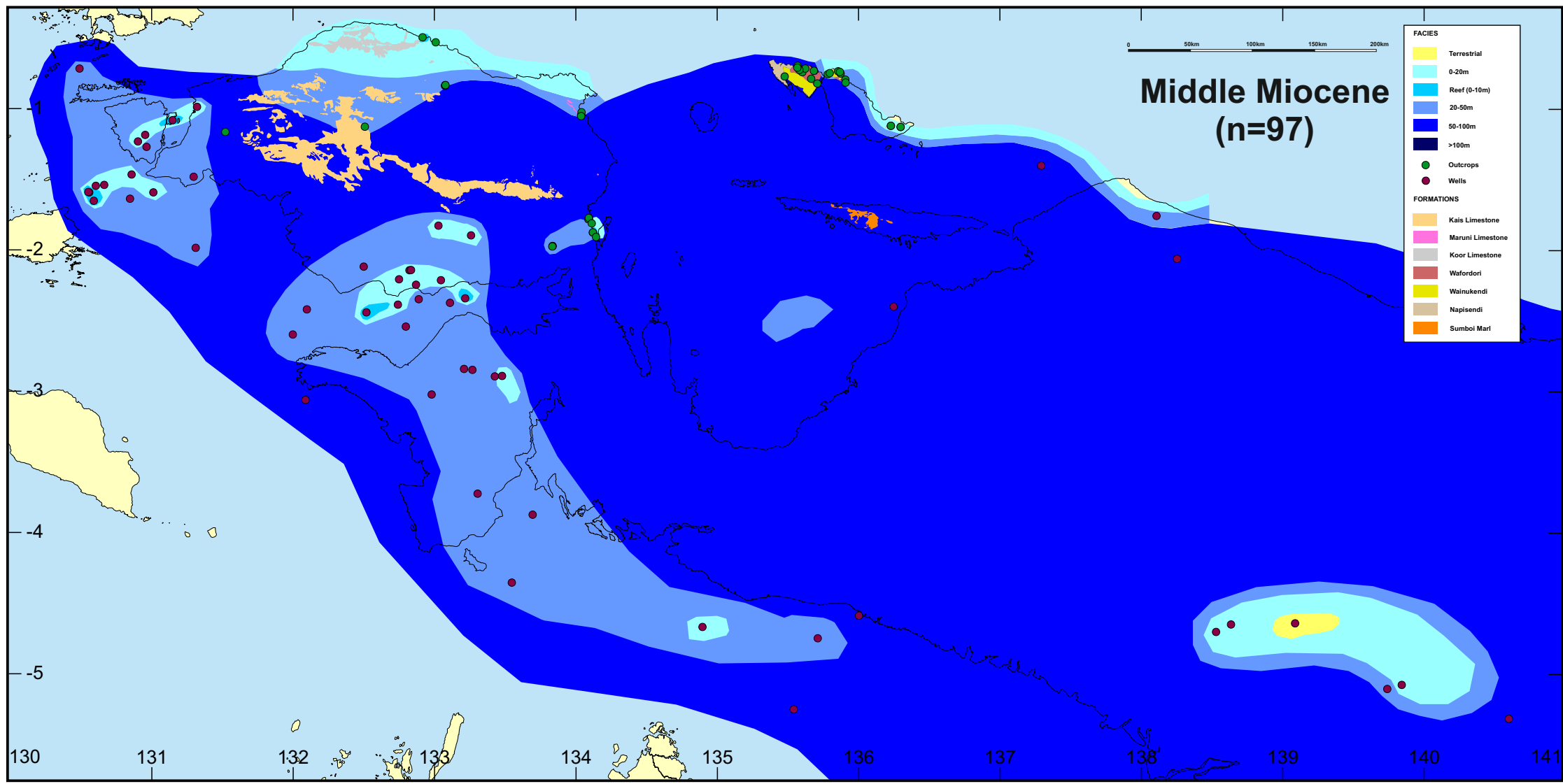


Figure 25

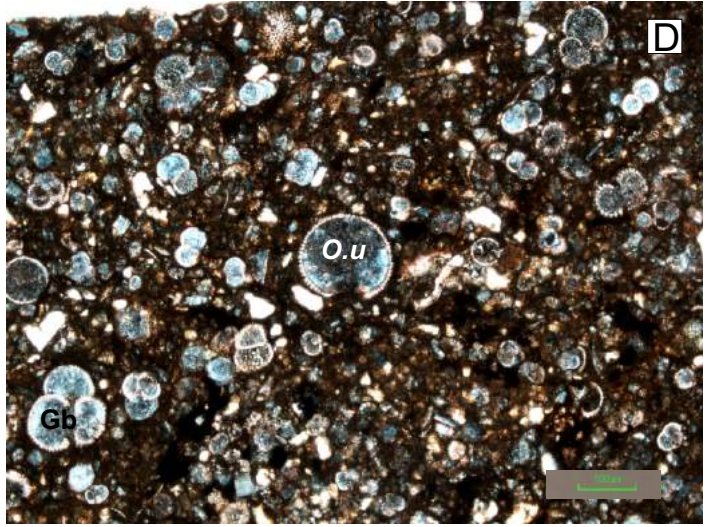
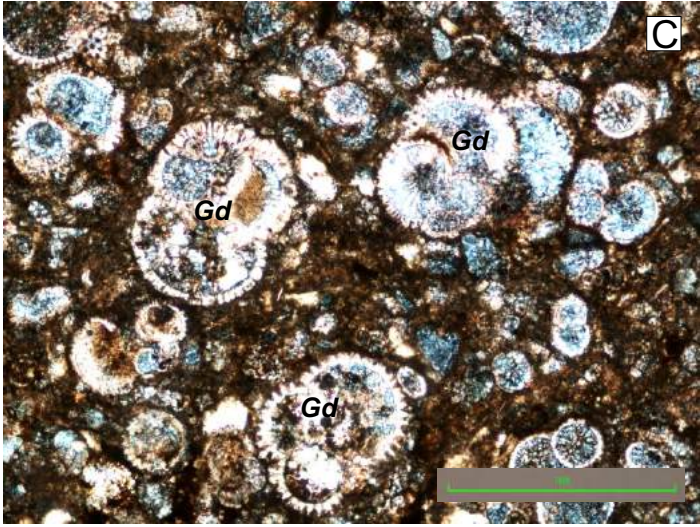
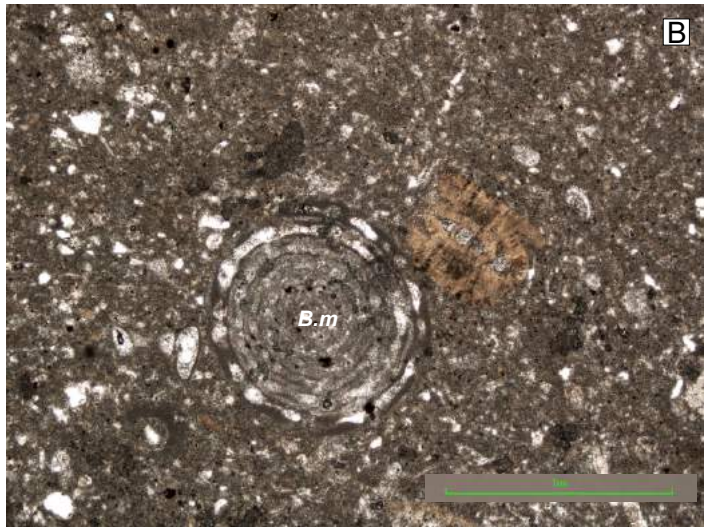


Figure 26

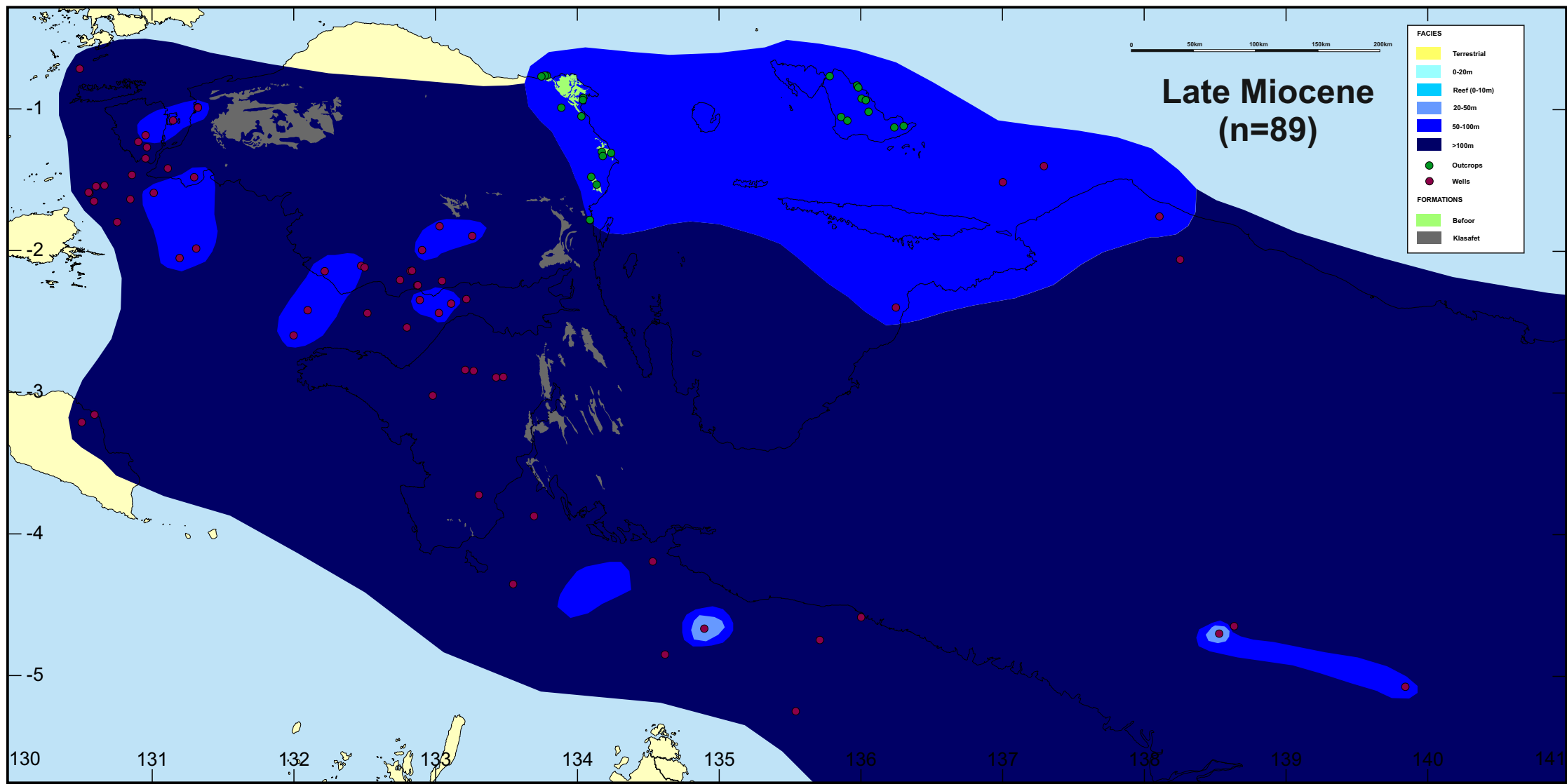


Figure 27

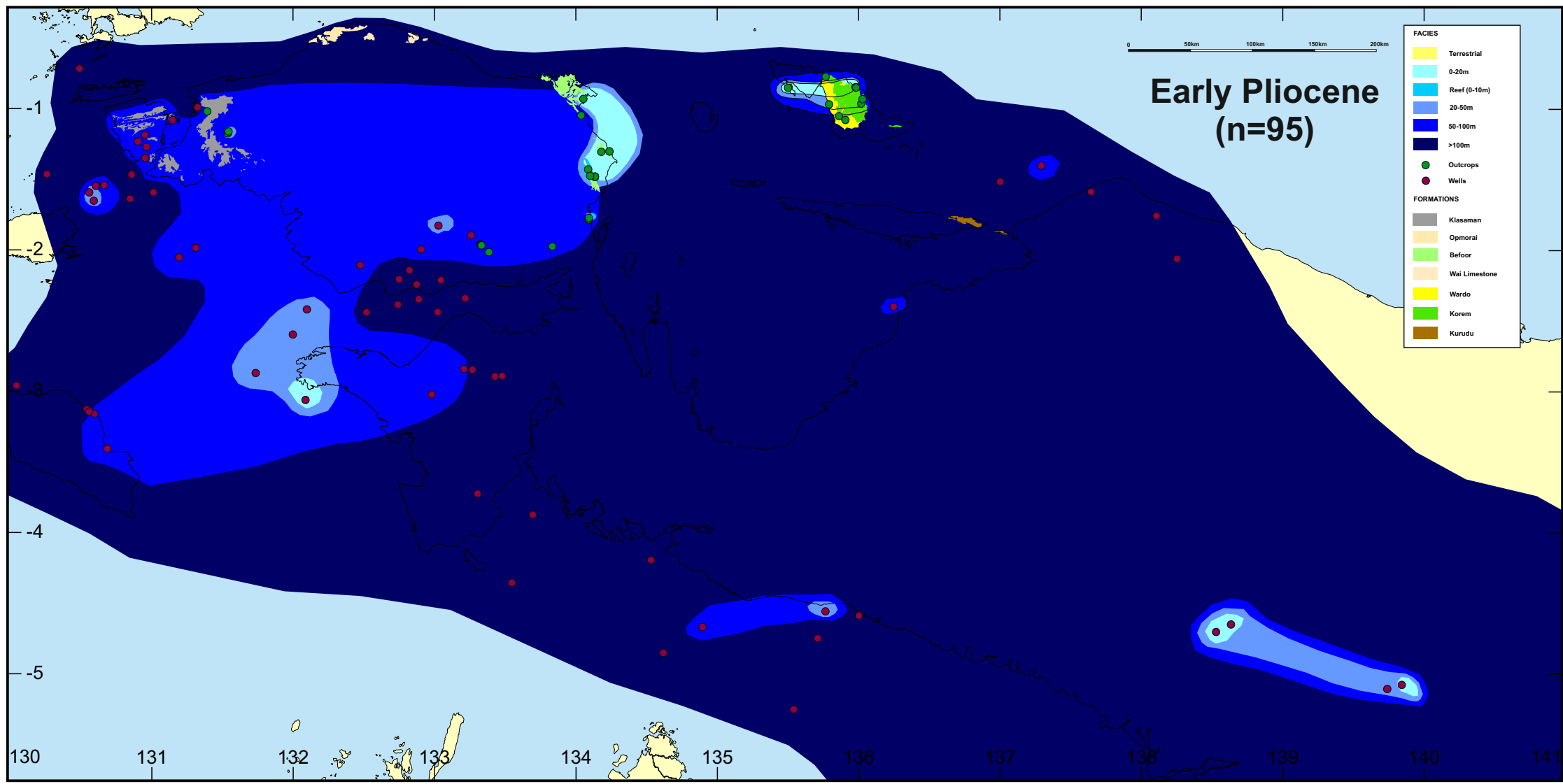


Figure 28

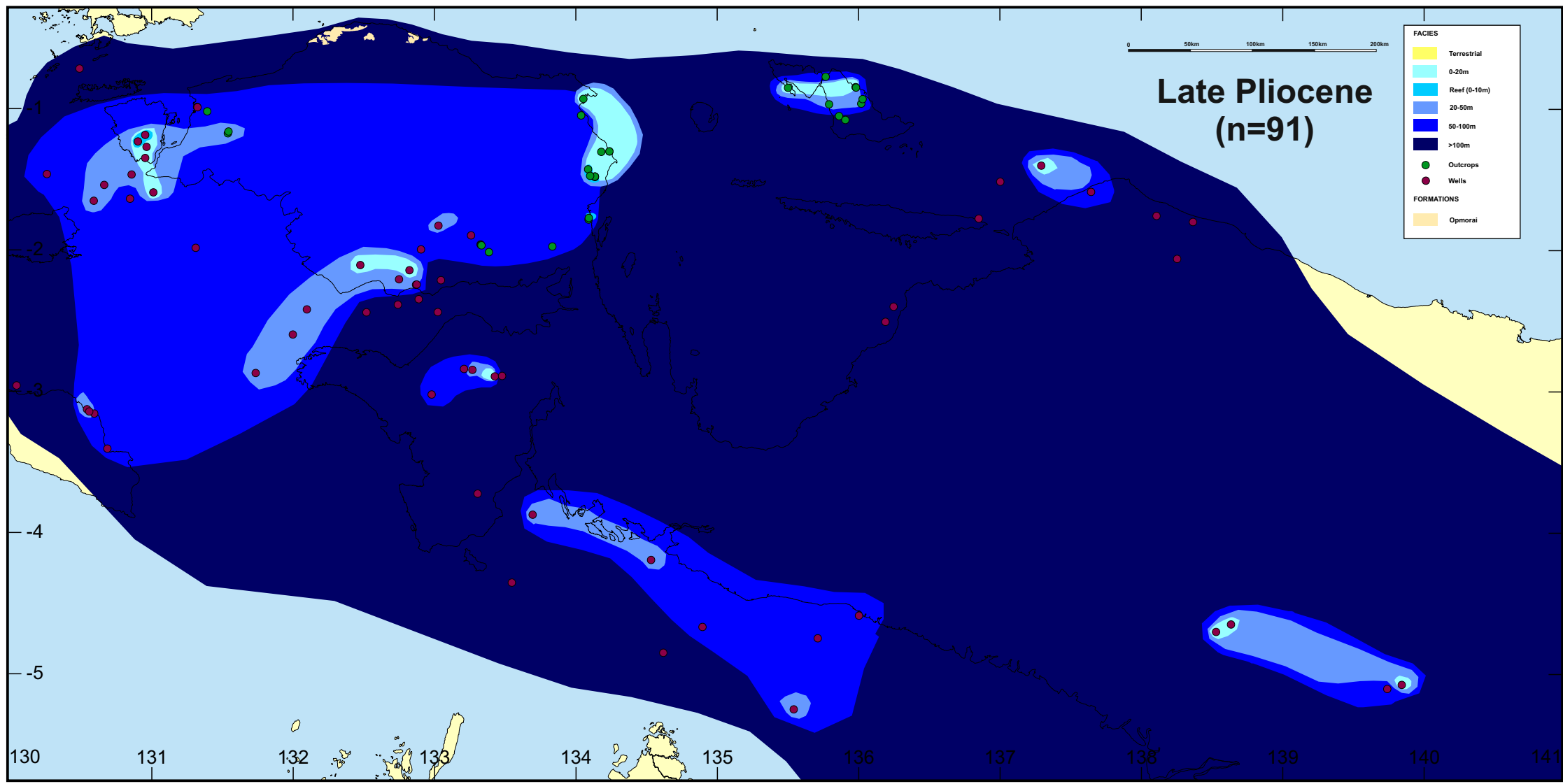


Figure 29

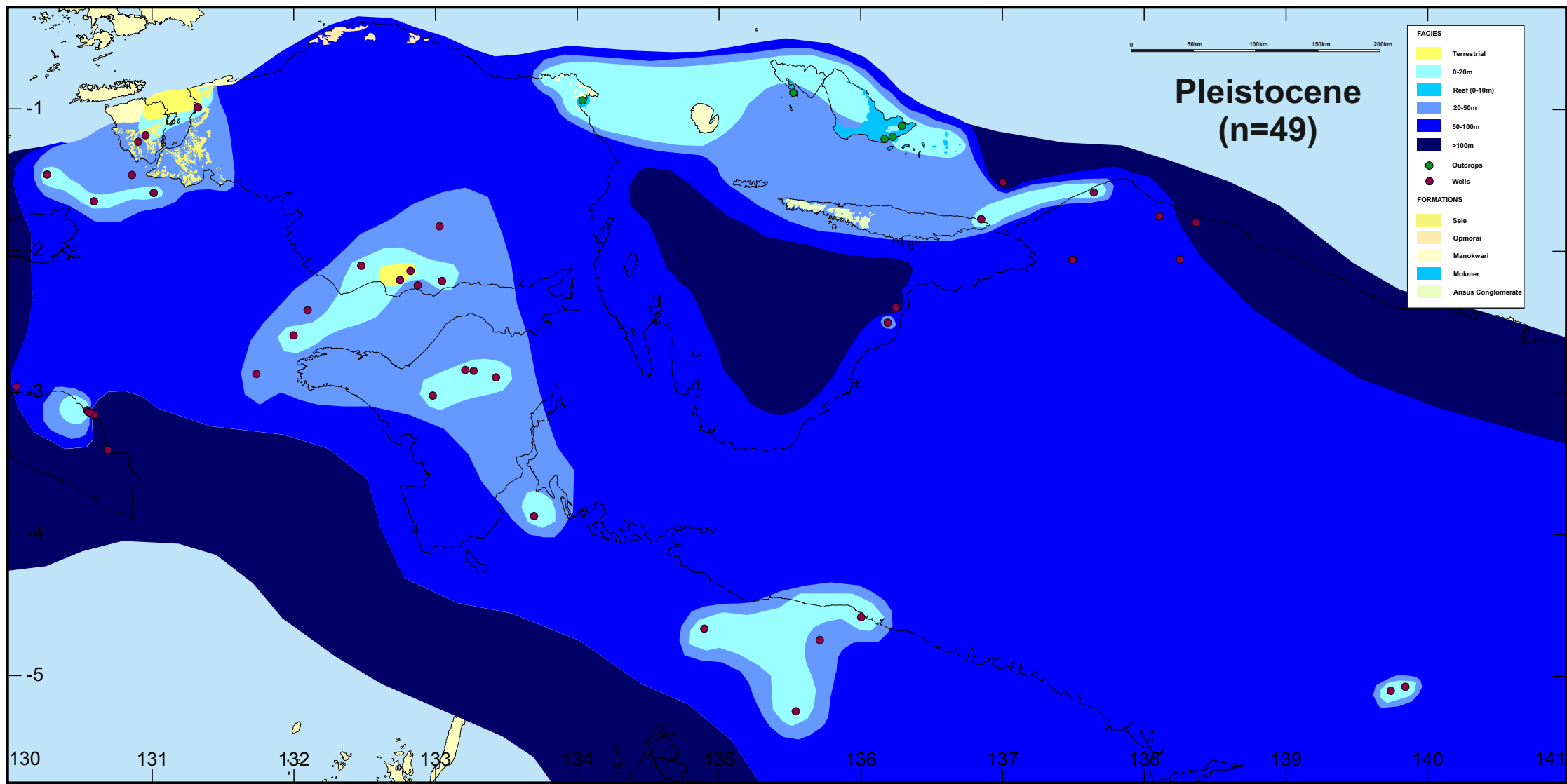


Figure 30